Published in final edited form as:
Toxicol Pathol. 2010 January ; 38(1): 9–36. doi:10.1177/0192623309354111.

Proceedings of the 2009 National Toxicology Program Satellite Symposium

Ute Bach[1], **James R. Hailey**[2], **Georgette D. Hill**[3], **Wolfgang Kaufmann**[4], **Kenneth S. Latimer**[5], **David E. Malarkey**[6], **Robert M. Maronpot**[7], **Rodney A. Miller**[8], **Rebecca R. Moore**[8], **James P. Morrison**[9], **Thomas Nolte**[10], **Matthias Rinke**[1], **Susanne Rittinghausen**[11], **Andrew W. Suttie**[5], **Gregory S. Travlos**[6], **John L. Vahle**[12], **Gabrielle A. Willson**[8], and **Susan A. Elmore**[6]

[1]Bayer HealthCare AG, Pharma Research Center, Wuppertal, Germany

[2]GlaxoSmithKline, Research Triangle Park, North Carolina, USA

[3]Integrated Laboratory Systems, Inc., Research Triangle Park, North Carolina, USA

[4]Experimental Toxicology and Ecology, BASF SE, Ludwigshafen, Germany

[5]Covance Laboratories Inc., Vienna, Virginia, USA

[6]National Toxicology Program and Cellular and Molecular Pathology Branch, National Institute of Environmental Health Sciences, National Institute of Health, Research Triangle Park, North Carolina, USA

[7]Maronpot Consulting, LLC, Raleigh, North Carolina, USA

[8]Experimental Pathology Laboratories, Inc., Research Triangle Park, North Carolina, USA

[9]Charles River Laboratories, Pathology Associates, Durham, North Carolina, USA

[10]Boehringer Ingelheim Pharma GmbH & Co. KG, Biberach/Riss, Germany

[11]Fraunhofer Institute for Toxicology and Aerosol Research, Hannover, Germany

[12]Lilly Research Laboratories, Eli Lilly & Co., Indianapolis, Indiana, USA

Abstract

The National Toxicology Program (NTP) Satellite Symposium is a one-day meeting that is held in conjunction with the annual Society of Toxicologic Pathology (STP) meeting. The topic of the 2009 Symposium was “Tumor Pathology and INHAND (International Harmonization of Nomenclature and Diagnostic Criteria for Lesions in Rats and Mice) Nomenclature.” The goal of this article is to provide summaries of each speaker’s presentation, including the diagnostic or nomenclature issues that were presented, along with a few select images that were used for voting. The results of the voting process and interesting points of discussion that were raised during the

Address correspondence to Susan A. Elmore, National Toxicology Program, Cellular and Molecular Pathology Branch, National Institute of Environmental Health Sciences, National Institute of Health, Research Triangle Park, NC 27709, USA; elmore@niehs.nih.gov.

presentation are also provided. A supplemental file with voting choices and voting results for each case presented at the symposium is available at http://tpx.sagepub.com/supplemental.

Keywords

NTP; satellite; symposium; INHAND; nomenclature

Introduction

The NTP Satellite Symposium was originally conceived and implemented by Dr. Robert Maronpot as a way to present current diagnostic pathology issues to the toxicological pathology community. The first Symposium was held in 2000, and the topic was "Establishing an NTP Database for Non-Neoplastic Lesions of Kidney and Urinary Bladder." There was no Symposium the following year, but in 2002, the NTP Satellite Symposium returned by popular demand and has been a consistent and highly regarded component of the annual STP meeting since that time. The history of meeting topics, dates, and locations is presented in Table 1. The Symposium has served as a forum to present and discuss lesions that are rare and interesting, present a diagnostic challenge, are controversial, or have nomenclature dilemmas. It was decided to hold the Symposium on the Saturday before the annual Society of Toxicologic Pathology (STP) meeting, as doing so would conveniently allow any interested STP registrants to attend. The Symposium has always been held at no cost to the participants, and attendance has been around 200 for the past few years.

The objective of the NTP Satellite Symposium has always been to provide continuing education on the interpretation of pathology slides, in terms of diagnostic or nomenclature dilemmas, that the bench pathologist may see from time to time. An equally important component of the Symposium has been to incorporate audience participation through anonymous voting and the generation of lively and productive conversation after the voting. The theme for the 2009 Symposium was "Tumor Pathology," corresponding with the STP meeting theme of cancer. We also included examples and discussion of International Harmonization of Nomenclature and Diagnostic Criteria for Lesions in Rats and Mice (INHAND) nomenclature as it pertains to neoplastic lesions. During each presentation, the speakers projected a series of lesion images on one screen with a choice of potential diagnostic choices listed on a separate screen. The members of the audience then voted anonymously with wireless keypads, and the voting results were displayed as bar graphs with percentages on the screen. After each voting session, the speakers sometimes presented additional data that may aid in the decision of diagnosis or choice of terminology, and then time was allowed for discussion. Occasionally, revotes were taken after the discussion period. In this article, the speakers have provided synopses of their presentations at the 2009 Symposium, including the diagnostic or nomenclature issues, a selection of images presented during the Symposium, voting choices, voting results, and discussion points.

Proliferative Adrenal Medullary Lesions in Rats

The first presentation, given by Dr. Georgette Hill, focused on proliferative adrenal medullary lesions in rats. An initial overview of the various lesions and primary diagnostic criteria was presented. Three diagnostic dilemmas were shown to Satellite Symposium participants. For case 1, a medullary mass (Figure 1A) with pleomorphic neoplastic cells (Figure 1B) was shown. Similar neoplastic cells were present in the periadrenal vasculature (Figure 1C). The diagnostic voting choices for case 1 were (1) adrenal medullary hyperplasia, (2) benign pheochromocytoma, (3) malignant pheochromocytoma, (4) complex pheochromocytoma, and (5) ganglioneuroma. Issues raised during the participant discussion of case 1 included the difficulty of identifying vascular invasion in a low-power image as depicted in Figure 1A, as well as whether vascular invasion is considered a feature of malignancy. Dr. Hill mentioned that, depending on the reference book used, the primary features of adrenal medullary malignancy are adrenal capsule invasion and the presence of distant metastasis (Hamlin and Banas 1990). Although neither of these was a feature of case 1, the majority of the participants (63% after a revote) agreed that vascular invasion and pleomorphic neoplastic cells classified this mass as a malignant pheochromocytoma, which was also the NTP choice.

A compressive medullary mass was shown for case 2 (Figure 1D). The diagnostic voting choices for case 2 were (1) adrenal medullary hyperplasia, (2) benign pheochromocytoma, (3) malignant pheochromocytoma, (4) neuroblastoma, and (5) hemangiosarcoma. The NTP choice, from a pathology working group (PWG) vote, was malignant pheochromocytoma because of the necrosis and presence of neoplastic cells in vessels within the tumor; however, the majority of the Satellite Symposium participants (49%) voted for neuroblastoma. Issues raised during audience discussion for case 2 included neoplastic cells appearing neuroblastoma-like owing to poor resolution on the screen and that neuroblastomas are rare neoplasms in the adrenal medulla of rats. For comparative purposes, a neuroblastoma (Figure 1E) is shown at a similar magnification (40X) to the adrenal medulla mass from case 2 (Figure 1F). The closely packed neuroblast-like cells with scant cytoplasm in Figure 1E were compared to the sheet of neoplastic chromaffin cells with abundant cytoplasm along the area of compression in Figure 1F.

A focal medullary lesion that did not compress the surrounding parenchyma was shown for case 3 (Figure 1G). The diagnostic voting choices for case 3 were (1) adrenal medullary hyperplasia, (2) benign pheochromocytoma, (3) malignant pheochromocytoma, (4) angiectasis, and (5) hemangiosarcoma. The majority of the Satellite Symposium participants (67%) voted for adrenal medullary hyperplasia, which was also considered the NTP choice via PWG vote.

Hepatocholangiocarcinoma: The Great Masquerader

The second presentation, by Dr. Rodney Miller, was based on the collaborative work of Drs. Rodney Miller, Rebecca Moore, and Gabrielle Willson and was titled “The Great Masquerader.” Dr. Miller’s discussion emphasized the various histomorphology patterns of hepatocholangiocarcinoma (HCCC) and thus the potential for diagnostic challenges.

After presentation of numerous images demonstrating the highly variable morphological patterns seen in the primary and metastatic lesions, a vote was taken, given the following diagnostic choices: (1) epithelioid hemangioendothelioma, (2) mesothelioma, (3) HCCC, (4) hepatocellular carcinoma, (5) atriocaval mesothelioma, and (6) hepatoblastoma. Hepatocholangiocarcinoma was the correct response and recorded a 57% vote. The other votes recorded were: epithelioid hemangioendothelioma (7%), mesothelioma (18%), hepatocellular carcinoma (2%), atriocaval mesothelioma (4%), and hepatoblastoma (12%). After the vote, a detailed presentation of HCCCs in the NTP database was given.

Hepatocholangiocarcinoma is a rare tumor with an overall incidence of less than 1% in male and female mice in the current NTP database. Hepatocholangiocarcinoma is defined as a combination of neoplastic hepatocytes and neoplastic biliary epithelial cells. In addition to the proliferative hepatocellular and biliary epithelial components, there may be a poorly differentiated cellular component that has a sarcomatous, anaplastic, and undifferentiated appearance. The variable histological morphology of the primary HCCC and the metastatic lesions may pose a diagnostic challenge. The purpose of this research and presentation was to describe the morphological features, incidence, and behavior of HCCC in B6C3F1 mice. The NTP historical database from 1982 to 2008 was reviewed for a diagnosis of HCCC in B6C3F1 mice (retrieved August 27, 2009, from the National Toxicology Program Web site: http://ntp-server.niehs.nih.gov). A total of 164 HCCCs (ninety-five male and sixty-nine female mice) from 74 two-year carcinogenicity studies were identified and reviewed.

Hepatocholangiocarcinoma occurred more commonly in males (58%) than in females (42%). Metastases were evident in 138 animals (84%) and often occurred in multiple sites. The sites most frequently observed to have metastatic lesions included lung (125/138, or 91%), mediastinum (104/138, or 75%), mesentery (80/138, or 58%), lymph nodes (71/138, or 51%), skeletal muscle (55/138, or 40%), kidney (47/138, or 34%), heart (46/ 138, or 33%), and pancreas (10/138, or 7%). Hepatocholangiocarcinomas were not considered to be treatment related in any study; however, in twenty-four of the seventy-four studies (32%), there was a concomitant treatment-related increase in hepatocellular tumors in one or both sexes. Although most of the NTP mouse control groups from this period did not have a diagnosis of HCCC, the highest incidence of spontaneous HCCC in any control group was as high as two of forty-nine for female controls and five of fifty for male controls.

All HCCCs reviewed in this study had a malignant hepatocellular component, as required by definition. The vast majority of HCCCs had small to large areas of necrosis and/or small to large areas of cystic spaces. The cystic areas had ill-defined epithelial linings or were partially lined by a flattened to cuboidal epithelium. Foci of proliferating epithelial cells forming ductal structures, representing the malignant biliary component, were often evident in close proximity to these areas of necrosis, or the cystic areas. Not infrequently, these foci were small and difficult to appreciate upon cursory examination (Figure 2A). Occasionally (about 16%), there were focal areas of proliferation of undifferentiated round to spindle cells in a loose fibrillar matrix within or adjacent to the malignant hepatocellular component (Figure 2B). It was not unusual to have transformation of neoplastic hepatocytes in the same proliferating hepatic cord into varieties of columnar epithelial cells to form ducts (Figure 2C).

The diagnostic challenge often began with the metastatic lesions. The metastatic lesions were often grossly visible, multifocal, and tan and occurred within the parenchyma of the tissue bearing the metastasis. The metastatic lesions also commonly extended to and occurred on serosal surfaces, where they stimulated serosal lining cells to react. If classical malignant hepatocellular components were present in the metastatic lesions along with the neoplastic duct-forming cells or the undifferentiated or spindle cells (Figures 2D and 2E), it stimulated the pathologist to return to the liver to confirm the presence of HCCC.

Commonly, the metastatic lesions contained only epithelial cells of the malignant biliary component (as was often the case in mesenteric metastases), an undifferentiated component, or sometimes a combination of both. Less commonly, the metastatic lesions contained the malignant hepatocellular component. The undifferentiated component was composed of nondescript round cells or spindle cells resembling a sarcoma. When this sometimes puzzling, but virtually pathognomonic, pattern of metastasis is seen, it often leaves the pathologist wondering whether the primary tumor is a carcinoma, a sarcoma, a mesothelioma, or a neoplasm of unknown histogenesis. The pathologist should then be stimulated to review the primary liver mass and evaluate it closely, looking for the diagnostic trilogy that leads to a diagnosis of HCCC: the malignant hepatocellular component, areas of necrosis or cystic degeneration, and the ducts of the malignant biliary component. The presence of a focal and undifferentiated or spindle cell proliferation in the liver mass adds even more strength to the argument and helps confirm that the primary tumor should be called an HCCC.

In summary, HCCC is a rare tumor in mice and is an aggressive tumor that metastasizes readily. The HCCC metastatic rate of 84% is much higher than that of hepatocellular carcinomas (about 23%) or hepatoblastomas (about 23%) (Turusov et al. 2002). Hepatocholangiocarcinoma was more commonly observed in male mice than in female mice in these NTP studies. Although it has been reported to be induced by chemicals such as benzidine dihydrochloride and N-2-acetoaminofluorene (Frith, Ward, and Turusov 1994), treatment-related HCCCs were not observed in the NTP dataset. Hepatocholangiocarcinoma can have a highly variable histological morphology, and careful evaluation of all features of the primary and metastatic lesions must be taken into account to render the correct diagnosis. Careful consideration must be given to hepatocellular proliferation, biliary epithelial proliferation, undifferentiated cell proliferation, cystic areas, and necrotic areas in the primary liver tumor and put into context with any combination of hepatocellular, biliary or undifferentiated cell proliferation in the metastatic lesions.

“Kneejerks” Welcomed: Diagnostic Value of Immunohistochemistry

Dr. Dave Malarkey of the NTP presented three cases that didn’t necessarily elicit a “kneejerk” diagnosis from participants, each one illustrating the diagnostic utility of various immunohistochemical markers. The first case was a brain mass from a male B6C3F1 mouse treated daily for ninety days with sodium dichromate dihydrate (Figures 3A and 3B). The voting choices were: (1) meningothelial meningioma, (2) transitional meningioma, (3) meningioma not otherwise specified (NOS), (4) malignant glioma, (5) histiocytic sarcoma, (6) inflammation, and (7) “other.” There was not a clear consensus audience vote, but the

two top choices were meningioma NOS (31%) and histiocytic sarcoma (25%). Dr. Malarkey then showed the abundance of F4/80, a macrophage-restricted cell surface gly-coprotein, by immunohistochemistry (IHC). The positive results indicate that this neoplasm was a histiocytic sarcoma. Histiocytic sarcoma, although considered an incidental finding in this case, is an important differential diagnosis in mice with meningial neoplasms.

The second case was a proximal urethral mass from a fourteen-month-old male B6C3F1 mouse that had been treated with 3,3′,4,4′-tetrachloroazobenzene (TCAB) by gavage (Figure 3C). Immunohistochemistry for p53 was used to illustrate positive staining of the neoplastic cells and for uroplakin III (Figure 3D) to characterize the neoplastic urothelium compared to overlying urethral epithelium. The voting choices were (1) adenocarcinoma of the prostate, (2) urethral transitional cell carcinoma, (3) urethral gland carcinoma, (4) squamous cell carcinoma, (5) carcinoma NOS, and (6) “other.” The two top audience voting choices were urethral transitional cell carcinoma (35%) and squamous cell carcinoma (33%). The NTP choice was urethral transitional cell carcinoma, an extremely rare neoplasm that was induced in >90% of treated male mice in this study, arising from the proximal urethra. Dr. Malarkey then presented several slides showing incidence data of carcinoma of the urethra in mice and rats and teaching diagrams of the male urogenital system and urethral carcinogenesis.

The third case presented by Dr. Malarkey was tissue from the cranial mediastinum (Figures 3E and 3F) of an eighteen-month-old female F344 rat with difficulty breathing and ataxia. The voting choices were (1) carcinosarcoma, (2) sarcoma NOS, (3) thymoma, (4) rhabdomyosarcoma, (5) sarcomatoid carcinoma, and (6) “other.” The clear best choice of the audience was thymoma (73%), and this was also the NTP choice. Additional slides were shown illustrating concurrent IHC positivity of the neoplasm for cytokeratin (Figure 3G) and desmin. A retrospective study of 244 thymomas in the NTP database showed only four having a myoid component.

Neoplasia in the Tg.AC Mouse

Drs. Andrew Suttie and Kenneth Latimer presented background neoplastic lesions in the Tg.AC mouse. The Tg.AC mouse is a transgenic mouse model used for carcinogenicity studies by dermal application. This model was developed from the FVB/N strain and carries an activated murine H-ras oncogene (Eastin et al. 1998). This transgene is linked to fetal ζ-globin promoter and SV40 polyadenylation/splice sequence. It responds to both genotoxic and nongentoxic carcinogens, resulting in a dramatic increase in cutaneous papillomas, keratoacanthomas, and squamous cell carcinomas (Eastin et al. 1998; Mahler et al. 1998). Additionally, the Tg.AC mouse develops odontomas and hematopoietic lesions, especially erythroleukemia, myelodysplasia, and lymphoma (Mahler et al. 1998; Trempus et al. 1998). The incidence of neoplasia from negative and positive control (12-*O*-tetradecanoylphorbol-13-acetate [TPA] treated) groups from five studies, totaling 110 animals per sex per group, is given in Table 2. Dr. Suttie presented lesions from the skin and head. The Symposium audience considered a typical skin neoplasm (Figure 4A) to agree on nomenclature, and the consensus vote was for papilloma. The audience was also shown a variety of skin lesions of varying severity to agree on a threshold of hyperplasia versus neoplasia to aid in consistent diagnosis of skin lesions in these carcinogenicity studies. An

example of one skin lesion is presented in Figure 4B. These lesions included epithelial hyperplasia, squamous papilloma, keratoacanthoma, and squamous cell carcinoma. The consensus of the audience was that lesions that had features of squamous papillomas represented the threshold for a diagnosis of neoplasia.

Additional skin lesions were then presented, including malignant transformation adjacent to a papilloma (Figure 4C). The audience considered images of masses from the oral cavity of Tg.AC mice (Figure 4D) and agreed that odontoma was the appropriate diagnosis. An oral cavity mass that did not present the typical appearance of an odontoma (Figure 4E) was considered by the audience, and the vote was divided, with diagnoses of osteosarcoma, ameloblastoma, and odontoma. The diagnosis of this neoplasm requires examination of multiple microscopic fields of view to discern all diagnostic features of the mass.

Dr. Latimer presented lesions from the hematopoietic system. A variety of chemically induced lymphohematopoietic disturbances have been reported in Tg.AC mice. Melphalan, an alkylating agent used in humans to treat multiple myeloma, produces dose-dependent lymphohematopoietic changes in bone marrow (hematopoietic cellular depletion, myeloid hyperplasia), spleen (cellular depletion in lymphoid follicles, lymphoid hyperplasia), and thymus (atrophy) (Eastin et al. 1998). Rotenone at high doses produces myelodysplasia, defined as having mixed features of inflammatory, hematopoietic, and neoplastic processes that involve multiple organs (Eastin et al. 1998). In myelodysplasia, eosinophils may also be a prominent feature (Eastin et al. 1998). Cyclosporine A, a fungal product used to treat graft-versus-host reactions in transplant patients, may produce malignant lymphoma when the drug is given at high doses (Eastin et al. 1998).

The audience considered lesions from the spleen, liver, and bone marrow (Figures 4F and 4G) from a Tg.AC mouse. The consensus vote of the audience was for lymphoma or myeloid leukemia, whereas the presenter’s diagnosis was erythroleukemia. Dr. Latimer agreed with the audience’s recognition of the lesion as hematopoietic neoplasia but mentioned that the determination of cellular lineage was critical in diagnosing the specific type of leukemia. Other locations where erythroleukemia was observed were presented, including lung (Figure 4H), kidney, ovary, pituitary, and brain. Both the lung and kidney had leukoaggregation within small blood vessels. There was considerable discussion concerning the diagnosis of erythroleukemia in the Tg.AC mouse. As originally described and published, the diagnosis of erythroleukemia was based on the examination of histologic sections in which nucleated red blood cells were admixed with undifferentiated blasts. Furthermore, the blasts had more cytoplasmic basophilia than lymphoblasts (Trempus et al. 1998). Dr. Latimer emphasized that a diagnosis of erythroleukemia should rely on anatomic pathology and clinical pathology findings. Histologic findings can confirm the presence of neoplasia and determine tissue and organ distribution, but they may not precisely classify the cellular lineage. Clinical pathology evaluation of laboratory data, blood smears, and bone marrow smears may be able to more precisely identify the cellular lineage. However, cytochemistry, IHC (in tissue section or by flow cytometry), and transmission electron microscopy may be necessary to classify some unusual cases of leukemia. Lastly, the audience considered a number of images of spleen with either hematopoietic neoplasia or

extramedullary hematopoiesis (EMH; Figure 4I) and voted on a diagnostic threshold for neoplasia versus EMH.

In summary, Dr. Latimer stated that “erythroleukemia” is a naturally occurring background hematopoietic neoplasm in Tg.AC mice. He also emphasized that cases of “erythroleukemia” in Tg.AC mice require additional study to verify the cell lineages and to determine whether other types of leukemia exist. Additional diagnostic techniques could include the use of cluster of differentiation (CD) antigens and transmission electron microscopy to determine the lineage(s) of these leukemias.

Hematopoietic Cell Proliferation versus Myleoid Hyperplasia

Dr. Greg Travlos presented two cases. The first involved an enlarged spleen with an excessive hematopoietic cell proliferation from an eighteen-month-old female C57BL/6NCrl mouse. Photomicrographs of histologic sections were presented (Figures 5A and 5B), and the audience was asked to choose from the following diagnostic choices: (1) normal, (2) granulocytic leukemia, (3) leukemoid response, (4) hematopoietic cell proliferation, (5) myeloid hyperplasia, and (6) need more information. Myeloid hyperplasia was the favored diagnostic selection (chosen by 45% of the respondents) over the preferred NTP terminology, hematopoietic cell proliferation (the runner-up choice, selected by 28% of the respondents). A lively discussion ensued regarding what should be considered the appropriate diagnostic terminology for such an excessive hematopoietic cell proliferation that effaces normal splenic architecture, especially in a species that normally has extramedullary hematopoiesis present in the spleen. No consensus was reached. A small number of respondents (15%) selected granulocytic leukemia as the diagnosis. Following the discussion, however, Dr. Travlos presented additional information regarding necropsy findings, including a severe, multifocal to coalescing, pyogranulomatous hepatitis, with intralesional Splendore-Hoeppli material and coccoid bacterial colonies (botryomycosis; *Staphylococcus aureus* was cultured from the lesion) (Figure 5C). This inflammatory lesion was used as explanation for the presence of the excessive hematopoietic cell proliferation within the spleen. Furthermore, presence of inflammation has been used as a criterion for the differentiation of granulocytic leukemia and myeloid hyperplasia of the spleen in the mouse (Long, Knutsen, and Robinson 1986); Dr. Travlos then presented an adaptation of the primary diagnostic criteria (Table 3).

For his second case, Dr. Travlos presented photomicrographs of Romanowsky-stained blood films; this was a nonvoting case. He presented examples of normal and polychromatophilic erythrocytes as a preface followed by protocol information regarding a four-day mouse study evaluating the effect of analgesia on postsurgery (partial hepatectomy) recovery. Dr. Travlos presented photomicrographs of four blood films representing each of the three treatment groups (no surgery/no analgesic-control, no surgery but treated with analgesic, surgery and treated with analgesic) and an age-matched normal animal that was not part of the study (Figure 5D). The discussion then focused on the excessive polychromasia observed in the study animals (regardless of treatment) and not found in the age-matched normal animal. For an explanation, Dr. Travlos returned to the study design, in which blood was collected three days prior to start and at day one of the study; blood for hematology was

collected at the end of the study. Thus, the bleeding of the mice twice (the reported collection amount was 50 mL/time point) within one week prior to the blood collection at study termination was sufficient to stimulate an erythropoietic response, resulting in increased release of immature erythrocytes and an increased polychromasia on the blood film. His take-home message was to consider study design and the potential effects that in-life blood collection may have on hematology parameters.

Introduction to the INHAND Initiative

As the sixth presenter, Dr. John Vahle, Chair of the Global and Editorial Steering Committee (GESC) gave a brief overview of the International Harmonization of Nomenclature and Diagnostic Criteria for Lesions in Rats and Mice (INHAND) project. The INHAND project involves efforts by members of the major Societies of Toxicologic Pathology—the Japanese Society of Toxicologic Pathology (JSTP), the British Society of Toxicologic Pathology (BSTP), the European Society of Toxicologic Pathology (ESTP), and the Society of Toxicologic Pathology (STP)—in an international collaborative effort to codify and publish uniform nomenclature for both proliferative and nonproliferative lesions in laboratory rodents (Vahle et al. 2009). Several features unique to this effort include (1) a truly international scope, (2) implementation of an open comment period allowing a wide group of toxicologic pathologists the opportunity to provide input, and (3) availability in a Web-based format. A global chairperson and members from each of the major societies of toxicologic pathology have formed “organ system working groups,” which have the responsibility to prepare nomenclature guidelines for both proliferative and nonproliferative lesions of rats and mice for their assigned organ system. The NTP Satellite Symposium presentations given by members of the organ system working groups were part of the effort to present various and challenging nomenclature issues to toxicologic pathologists for helpful input and discussion.

Diagnostic Features of “Glioma Type“ Tumors

Dr. Wolfgang Kaufmann, Chair of the INHAND Central Nervous System Working Group, presented a talk on tumors that originate from the brain with a special focus on “glioma type” tumors. Examples from cases of a malignant and a benign oligodendroglioma, a malignant astrocytoma, and a malignant pineal gland tumor (all found in Wistar rats from long-term studies) were presented, as well as a malignant mixed glioma found in a C57BL mouse from a three-month subchronic study. Assessment of tumors was based on World Health Organization (WHO) nomenclature for rodents (Krinke et al. 2001; Mohr 1994), which is also the baseline for the revision of the new INHAND initiative. An overview of the main characteristic criteria was given after voting on the tumors, and special techniques for diagnostics (e.g., glial fibrillary acidic protein [GFAP] stain that is negative in rodent astrocytomas) were summarized (Tables 5–9). The oligodendroglioma that was originally diagnosed as “malignant” was a large but well-circumscribed lesion that spread over multiple major brain areas, showed necrosis and hemorrhages (Figure 6A), and had the characteristic feature of atypical capillary endothelial hyperplasia (Figure 6B). The “benign” oligodendroglioma was a small and circumscribed lesion that was confined to one major brain area (Figure 6C) and often showed a “honeycomb” or “fried-egg” cell pattern (Figure

6D). This pattern is essentially artificial and a result of delayed fixation of the brain in the classical routine studies. The “malignant” variant of astrocytoma generally has round to fusiform cells, indistinct cell borders (not well circumscribed), cellular atypia, and pleomorphism. Cells may exhibit protoplasmic or fibrillary differentiation and prominent round or oval nuclei (Figure 6E). Necrosis with pseudopalisading was shown as one characteristic feature (Figure 6F). The mixed glioma of the mouse displays both proliferative astrocytoma and oligodendroglioma-like areas (Figure 6G). The term “mixed” (glioma) is used in all cases in which at least 20% of the tumor shows either one of the characteristic patterns of astrocytomas or oligodendrogliomas.

The last case shown by Dr. Kaufmann is an important differential diagnosis for brain tumors. This tumor developed in the midline of the cerebrum but is derived from the pineal gland. The malignant pinealoma often expands by invasion into the adjacent brain tissue and is highly cellular, rich in mitotic figures, and pleomorphic (Figure 6H).

Some principal controversy was raised concerning the use of “benign” and “malignant” for the glial tumors of the central nervous system. This use for rodents differs from the use in domestic animals and humans, in which “low-grade” up to “high-grade” malignancies are defined for all gliomas (Kleihues and Cavenee 2000). The fact that the size of the brain tumor may be far less relevant than the topography where the tumor arises was also addressed. The terms “benign” and “malignant,” according to the WHO nomenclature for rodents, are not used to give information on prognostic outcome or biological behavior but rather are used with respect to the cell morphology/architectural appearance of the tumors only at the time of diagnosis.

Unusual Proliferative Lesions of the Lung—A Diagnostic Dilemma

Dr. Rick Hailey presented images from a two-year carcinogenicity (gavage) study conducted in CD-1 mice with a control and three dose groups. There was a high (>25%) incidence of hemangiosarcomas (and a few hemangiomas) only in female mice at the high dose. Hemangiosarcomas occurred most commonly, and sometimes only, in the lung, which is a rare site for primary hemangiosarcoma (Figures 7A–D). However, hemangiosarcomas also occurred in the liver, spleen, and uterus. The Symposium participant consensus for the pulmonary lesions was hemangiosarcoma. In addition to obvious hemangiosarcomas, there was a broad spectrum of presumably nonneoplastic lesions. Ranging from very small to large and complex, these lesions consistently comprised eosinophilic fibrinous material, fibrosis, and hypertrophied spindled cells (Figures 7E–I). These lesions presented the following diagnostic challenges: (1) determining whether they were preneoplastic, (2) consistently identifying the morphologic criteria indicative of the diagnostic threshold between presumed pre-neoplasia and neoplasia, and (3) determining the best diagnostic term(s) for this spectrum of lesions. In Figure 7J, neoplastic transformation has occurred in the upper portion of the lesion, whereas there is less certainty with regard to the lower portion. Lacking biological information, angiomatous hyperplasia/ fibrosis, although clearly imperfect, was used to capture the spectrum of morphological change considered nonneoplastic and possibly preneoplastic in this study. Symposium participants voted on Figure 7K with diagnoses of angiomatous hyperplasia/ fibrosis (16%), angiomatous

hyperplasia (15%), hemangioma (13%), hemangiosarcoma (2%), endothelial hyperplasia (2%), spindle cell hyperplasia/fibrosis (1%), and other (50%). There was no consensus on the best diagnostic term(s) for this particular lesion.

Non-Granular Cell Meningiomas in Rodents

Dr. Jim Morrison discussed non-granular cell meningiomas in rodents. As a group, meningiomas have a high degree of morphological diversity, particularly in humans and domestic animals, and Dr. Morrison's presentation began with an overview of meningioma histomorphology and classification. The most recent WHO classification of tumors of domestic animals included nine meningioma morphological subtypes (Table 10) (Koestner et al. 1999); however, the list of morphological subtypes currently recognized in the rodent literature is more limited, consisting of meningotheliomatous, fibrous, anaplastic/undifferentiated, and granular cell (Dagle, Zwicker, and Renne 1979; Krinke et al. 2000; Mitsumori, Maronpot, and Boorman 1987; Morgan et al. 1984; Solleveld and Boorman 1990; Solleveld, Gorgacz, and Koestner 1991; Yoshida et al. 1997).

Dr. Morrison's first case was from a B6C3F1 mouse from an NTP two-year toxicity study; it was not related to the administration of test article (Figures 8A and 8B). Dr. Morrison's preferred diagnosis for the case was a myxoid malignant meningioma, and the majority (74%) of the audience agreed. It has long been recognized that mouse meningiomas could be predominantly myxoid (Krinke et al. 2001), but historically, these tumors have been classified as a variant of the fibrous meningioma phenotype. However, it seems that the frequency with which this morphology occurs in rodents has been underappreciated. In a recent retrospective review of mouse meningiomas from the archives of the National Toxicology Program performed by Dr. Morrison and Dr. Dave Malarkey of the NIEHS, twelve of nineteen (63%) neoplasms were myxoid in morphology (two of four benign, ten of fifteen malignant). Dr. Morrison recommended adding the morphological subtype "myxoid meningioma" to the list of recognized morphologies of meningiomas in the mouse (Table 11).

Dr. Morrison's second case was from a Fischer 344 rat from an NTP two-year toxicity study, but the case was also not related to treatment (Figure 8C and 8D). Dr. Morrison's preferred diagnosis for this case was a "psammomatous meningioma" based on the presence of numerous foci of hyalinized collagen and mineralization (psammaoma bodies) throughout the neoplasm. The majority (74%) of the audience agreed. Psammoma bodies are not a common feature of rodent meningiomas (Solleveld, Gorgacz, and Koestner 1991), and psammomatous meningiomas have not been previously reported in the literature. The neoplasm shown in Dr. Morrison's presentation was one of two psammomatous meningiomas recently identified in the NTP archives by Dr. Morrison in the Fischer 344 rat. Dr. Morrison concluded by recommending that "psammomatous meningioma" be added to the list of recognized meningioma morphological subtypes in rats (Table 12).

Proliferative Lesions in the Stomach

The tenth speaker, Dr. Thomas Nolte, presented diagnostic issues of proliferative lesions in the stomach of control animals from the Registry of Industrial Toxicology Animal Data

(RITA) working group. The first in this series of three cases was a proliferation of the squamous epithelium in the forestomach of a female Wistar rat sacrificed at termination of a carcinogenicity study. The lesion was slightly elevated from the surrounding mucosa but lacked a stromal stalk, and thus mimicked a “sessile papilloma” (Figure 9A). The epithelium was moderately thickened, predominantly by prominent rete pegs. These rete peg structures were composed primarily of basal and prickle cells and, to a lesser extent, of cells of the stratum granulosum (Figure 9B). The superficial part of the lesion showed a slightly thickened stratum granulosum and normal keratinization. The voting choices given were (1) no abnormality detected—tangential section of the limiting ridge; (2) hyperplasia, squamous cell; (3) acanthosis; (4) hyperplasia, basal cell; and (5) papilloma, squamous cell. Basal cell hyperplasia was the diagnosis preferred by the audience (47%). The majority of a RITA panel preferred “hyperplasia, squamous cell,” because it was considered that all epithelial layers were involved and exaggerated rete peg formation does occur in squamous cell hyperplasia; this opinion was shared by 29% of the audience. In the discussion, the point was made that the proliferative component, namely, the rete peg structures, consisted predominantly of basal cells supporting the diagnosis of basal cell hyperplasia in this borderline case.

Similar to the first case, the second case that Dr. Nolte presented showed a proliferation in the forestomach of a female Wistar rat sacrificed at the end of a carcinogenicity study. The focal and flat mucosal lesion was slightly elevated from the surrounding unaltered mucosa (Figure 9C). Stratum granulosum and corneum were developed in an orderly fashion, overlying prominent hyperplastic basal cells. These hyperplastic cells formed tightly packed papillary projections, giving the appearance of a nearly solid proliferation of basal cells (Figure 9D). The same voting choices were offered as for case 1, with the exception that option 5 was modified to “sessile or inverted papilloma.” The audience voted almost unanimously (91%) for “hyperplasia, basal cell,” which was in line with the diagnosis of a RITA panel.

With case 3, Dr. Nolte showed a proliferative lesion of the glandular stomach of a male Wistar rat from a carcinogenicity study. This kind of lesion is occasionally found in Wistar and Sprague-Dawley rats from control groups of carcinogenicity studies. The lesion is always located close to the limiting ridge (Figure 9E). The hallmark of this lesion is the occurrence of a single focus or few foci of basal cell proliferations within the glandular mucosa (Figure 9F). The following voting choices were given: (1) no abnormality, part of nonglandular mucosa (rete pegs); (2) ectopic squamous epithelium; (3) hyperplasia, basal cell; (4) metaplasia, basal cell; and (5) tumor, basal cell, benign. The RITA group considers this type of lesion proliferative and currently calls it “hyperplasia, basal cell.” According to alternative histogeneses, the terms “metaplasia, basal cell,” or a proliferation of ectopic forestomach epithelium, were also discussed. These thoughts and the uncertainties about the histogenesis were shared by the audience. “Ectopic squamous epithelium” was favored by 35%, and 42% chose “hyperplasia” or “metaplasia, squamous cell.” During the discussion, colleagues voting for “ectopic squamous epithelium” emphasized the proliferative component of this lesion.

Pulmonary Mucous Cell Proliferation

Expression of this protein is predominantly in the Clara cells in the control rat. Dr. Susanne Rittinghausen, GESC liason to the INHAND Respiratory System Working Group, gave a presentation on pulmonary mucous cell proliferation compared to the expression of this protein predominantly in the Clara cells in the control rat. The case presented for voting was tissue from a Wistar rat that had been exposed to 45 mg of diesel engine exhaust via intratracheal instillation in a carcinogenesis bioassay. This animal was sacrificed moribund at 114 weeks of age. At necropsy, there was a 10 mm dark red, firm lung mass. A series of twelve images were shown (Figures 10A–D), and the voting choices were: (1) bronchiolo-alveolar carcinoma, (2) bronchial adenocarcinoma, (3) bronchiolo-alveolar hyperplasia, (4) exaggerated mucous cell metaplasia, (5) hypermucinosis, and (6) alveolar lipoproteinosis. The audience's favorite diagnosis was exaggerated mucous cell metaplasia (60%), and this was Dr. Rittinghausen's choice as well. The diagnostic features of pulmonary mucous cell metaplasia were then presented to the audience (Table 13). Differential diagnoses of alveolar proteinosis, bronchiolo-alveolar hyperplasia, bronchial adenocarcinoma, and bronchiolo-alveolar carcinoma were then discussed, with images illustrating diagnostic features. Dr. Rittinghausen then presented images of PAS positive material (Figure 10E) and PCNA IHC (Figure 10F) within the lesions of exaggerated mucous cell metaplasia. There was then discussion of pathogenesis and cell of origin. Dr. Rittinghausen suggested that the Clara cells and/or alveolar type II epithelial cells undergo mucous cell metaplasia. CD54 (ICAM-1) IHC was then used to illustrate positive cells within the lesion in the diesel-exposed rat (Figure 10G) and the absence of staining in the control tissue. Images of Clara cell secretory protein IHC were used to illustrate the expression of this protein within the pulmonary interstitial tissue in the treated rat (Figure 10H) compared to the

Granular Cell Lesions in the Female Genital Tract

The twelfth presentation was a collaborative effort between Dr. Ute Bach, a member of the INHAND Female Reproductive System Working Group, and Dr. Matthias Rinke. In this presentation, Dr. Bach showed the diagnostic features used in the RITA database for the different granular cell lesions as they occur in the female genital tract. She presented the case of a granular cell hyperplasia in the uterine cervix of a female Wistar rat that was sacrificed at the end of a two-year carcinogenicity study. At necropsy, this lesion was recorded as a single beige and hard nodule with a diameter of approximately 1 cm. Histologically, this preneoplastic lesion was characterized by clusters of cells with abundant eosinophilic cytoplasm and small basophilic nuclei without showing any compression of the surrounding tissue. There was no newly formed collagen between the cells. The normal tissue architecture was preserved (Figures 11A and 11B). For the voting procedure, the following diagnoses were given: (1) granular cell aggregates, (2) granular cell hyperplasia, (3) benign granular cell tumor, and (4) malignant granular cell tumor. Forty percent of the audience voted for hyperplasia, and 44% voted for the benign tumor. During the following discussion, this question arose: if the lesion caused a macro-scopically evident finding, is this reason enough to call it a benign tumor? In general, granular cell lesions consist of a uniform population of cells with a granular eosinophilic cytoplasm and a small basophilic nucleus. They are diastase resistant, PAS positive, and, in the female genital tract, usually

positive for S100 protein, which give reason for a neuroecto-dermal—most likely Schwann cell—origin.

Dr. Bach then presented the diagnostic criteria for the other lesions as they are currently used for the RITA database. In contrast to hyperplasia, the benign granular cell tumor is usually a circumscribed, well-demarcated mass with prominent, newly formed interstitial collagen causing compression of the surrounding tissue (Figures 11C and 11D). The malignant variant is known only from literature data (Markivits and Sahota 2000). Dr. Bach pointed out that until now, no such tumor is stored in the RITA database. Also, no one from the audience had ever seen the malignant form. According to the literature, the tumor shows pleomorphism, necrosis, and an increased nucleus-to-cytoplasm ratio. Mitotic figures are not common. The described malignant tumor therefore seems to differ from its benign counterpart only by its morphology. Moreover, it shows the same biological behavior without any regional or distant metastasis. As a nonproliferative lesion, the granular cell aggregates present as small cell clusters with at least three to five cells without any disturbance of the normal tissue architecture (Figure 11E). At the end of her talk, Dr. Bach stated that in the RITA database, among all granular cell lesions in the female genital tract, the benign granular cell tumor is the most frequent finding. However, in general, all granular cell lesions are rather rare occurrences (<0.6%) in the female genital tract.

Nodular Hyperplasia Revisited

Dr. Robert Maronpot introduced the topic of proliferative liver lesions in rodents, with a brief review of the nomenclature terms from the 1960s to the present time (Maronpot et al. 1986; Narama et al. 2003; Squire and Levitt 1975; Stewart et al. 1980). Primary diagnostic features of rat hepatoproliferative lesions show considerable overlap, especially for regenerative hyperplasia secondary to hepatotoxicity (synonym: nodular hyperplasia) and the newly recognized large hyperplastic lesion not associated with obvious hepatotoxicity. The latter was presented at the NTP Satellite Symposium in 2008, and representative examples were shown by Dr. Maronpot, who indicated that there was no clear consensus on this “nonregenerative” hyperplasia at the 2008 meeting (Figures 12A–D). In the discussion that followed, Dr. Taki Harada indicated that the “nonregenerative” hyperplastic lesion occurs in both treated and control rats. According to Dr. Harada, these lesions differ from large foci of cellular alteration. They lack phenotypic alteration, merge with surrounding tissue without compression, contain multiple portal triads, and are more PCNA positive than adjacent unaffected hepatic parenchyma. Dr. Maronpot commented that in years past, similar large lesions were considered “areas of cellular alteration” and classified along with foci of cellular alteration.

The term “nonregenerative” hyperplasia is currently under consideration by the INHAND liver nomenclature committee. The current opinion is that although regenerative hyperplasia is an appropriate diagnostic term that reflects a nodular proliferative response secondary to hepatotoxicity, “nonregenerative” is an inappropriate modifier, and a simple diagnosis of hyperplasia or focal hyperplasia would be suitable in the absence of hepatotoxicity. The INHAND liver nomenclature group will further discuss the most appropriate terminology for this diagnostic entity.

Since similar nodular hepatocellular proliferative lesions have been seen in mice and have been the subject of considerable debate, Dr. Maronpot presented three cases from B6C3F1 mice. Case 1 was a discrete, solitary hepatic nodule seen grossly in a male mouse treated with a low dose of Goldenseal Root Powder (Figures 12E and 12F). There was no obvious evidence of hepatotoxicity. The voting results were about equal for focal hyperplasia and hepatocellular adenoma. At a previous NTP Pathology Working Group (PWG), the favored diagnosis was hepatocellular adenoma. The difficulty in this case was the presence of multiple portal triads within the nodular lesion. According to conventional dogma, portal triads only very rarely occur in hepatocellular adenomas.

Case 2 was from a male B6C3F1 mouse in the mid-dose group of the Goldenseal Root Powder study. As in the previous case, a discrete nodular proliferation was present and contained portal triads (Figures 12G and 12H). Two other 2-mm nodules were seen grossly in this mouse. The votes favored focus of cellular alteration, and this was also the primary diagnosis in a previously conducted NTP PWG. As in case 1, there was no obvious evidence of hepatotoxicity.

Case 3 was one of three large masses seen grossly in a male mouse that received the low dose of Goldenseal Root Powder. This lesion protruded above the natural surface of the liver (Figure 12I) and had portal areas that were present within as well as at the outer margins of the lesion. The voting clearly favored hepatocellular adenoma. It is interesting that the NTP PWG on this lesion was equally split between focus of cellular alteration, hepatocellular adenoma, and nodular hyperplasia.

During the discussion of each of these cases, Dr. Maronpot emphasized that in contrast to traditional dogma, portal areas can be present in foci of cellular alteration, nodular hyperplasia with or without associated hepatotoxicity, and hepatocellular adenomas. Consequently, one should not use their presence or absence as a definitive diagnostic criterion for these specific diagnoses.

Summary

The NTP Satellite Symposium this year was a mixture of cases that presented either tumor pathology or INHAND nomenclature issues. Tumor pathology was chosen as the theme to coincide with the concurrent STP 28th Annual Symposium theme of “Cancer.” Challenging neoplastic lesions from a variety of organ systems were presented and discussed. In addition, INHAND nomenclature issues were presented as a way to provide a platform for the timely and important discussion of some particular cases that the INHAND Organ Working Groups were currently, or soon to be, discussing. Discussion and input from the toxicologic pathology community was requested and important for the Organ Working Groups to consider while preparing their draft nomenclature documents. As in previous years, the NTP Satellite Symposium was well attended, and audience participation was exceptional.

Supplementary Material

Refer to Web version on PubMed Central for supplementary material.

Acknowledgments

The authors wish to acknowledge Dr. Gordon Flake and Dr. Mark Hoenerhoff for their careful review of this article. Appreciation also goes to Eli Ney for her unique and creative artwork as well as her technical expertise in formatting the speakers' PowerPoints, and to both Eli Ney and Beth Mahler for their assistance during the Symposium and for manuscript image preparation. The authors also wish to thank Sue Pitsch, Krystal Gully, Elaine Adams, and Tierre Miller from Association Innovation and Management, Inc. for their valuable help with meeting planning, organization, and advertising, as well as Connie Cox, Chris Summerlin, Paul Allen, Gerald Burris, Armond Middleton, Nita Allen, Lou Ellis, and Dimas Pinzon from Capital Audio Visuals, Inc. for their exemplary assistance and technical help. Also integral to the success of this meeting was the security provided by Bill Stoeffler of Stoeffler Group, LLC.

This research was supported (in part) by the Intramural Research Program of the NIH, National Institute of Environmental Health Sciences.

Abbreviations

BSTP	British Society of Toxicologic Pathology
CD	cluster of differentiation
EMH	extramedullary hematopoiesis
ENU	ethylnitrosourea
ESTP	European Society of Toxicologic Pathology
F344	Fischer 344
GESC	Global and Editorial Steering Committee
GFAP	glial fibrillary acidic protein
HCCC	hepatocholangiocarcinoma
H&E	hematoxylin and eosin
ICAM	intercellular adhesion molecule
IHC	immunohistochemistry
INHAND	International Harmonization of Nomenclature and Diagnostic Criteria for Lesions in Rats and Mice
JSTP	Japanese Society of Toxicologic Pathology
NOS	not otherwise specified
NTP	National Toxicology Program
PAS	periodic acid-Schiff
PCNA	proliferating cell nuclear antigen
PWG	pathology working group
RITA	Registry of Industrial Toxicology Animal-Data
STP	Society of Toxicologic Pathology
TCAB	3,3′4,4′-tetrachloroazobenzene
TPA	12-*O*-tetradecanoylphorbol-13-acetate

WHO World Health Organization

References

Dagle GE, Zwicker GM, Renne RA. Morphology of spontaneous brain tumors in the rat. Vet Pathol. 1979; 16:318–324. [PubMed: 442462]

Eastin WC, Haseman JK, Mahler JF, Burcher JR. The National Toxicology Program evaluation of genetically altered mice as predictive models for identifying carcinogens. Toxicol Pathol. 1998; 26:461–473. [PubMed: 9715504]

Frith, CH.; Ward, JM.; Turusov, VS. Tumours of the liver. In Pathology of Tumours in Laboratory Animals. In: Turusov, VS.; Mohr, U., editors. Tumours of the Mouse. 2nd ed.. Vol. Vol. 2. Lyon, France: IARC Scientific Publications No. 111; 1994. p. 223-269.

Hamlin, MH.; Banas, DA. Adrenal gland. In: Boorman, GA.; Eustis, SL.; Elwell, MR.; Montgomery, CA.; MacKenzie, WF., editors. In Pathology of the Fischer rat: Reference and Atlas. San Diego, CA: Academic Press, Inc; 1990. p. 501-518.

Kleihues, P.; Cavenee, WK., editors. Pathology and genetics of tumours of the nervous system,. Lyon, France: IARC Press; 2000. World Health Organization classification of tumours; p. 1-314.

Koestner, A.; Bilzer, T.; Fatzer, R.; Sculman, FY.; Summers, B.; Van Winkle, TJ. World Health Organization Histological Classification of Tumors of the Nervous System of Domestic Animals. Schulman, ., editor. Washington, DC: Armed Forces Institute of Pathology; 1999. p. 1-71.

Krinke GJ, Kaufmann W, Mahrous AT, Schaetti P. Morphologic characterization of spontaneous nervous system tumors in mice and rats. Toxicol Pathol. 2000; 28:178–192. [PubMed: 10669006]

Krinke, GJ.; Fix, A.; Kaufmann, W.; Ackerman, LJ.; Garman, RH.; George, C.; Jortner, BS.; Leininger, JR.; Mitsumori, K.; Morgan, KT.; Paulson, I.; Robinson, M. Central nervous system. In: Mohr, U., editor. In International Classification of Rodent Tumors: The Mouse. Berlin: Springer; 2001. p. 323-345.p. 340-343.

Long RE, Knutsen G, Robinson M. Myeloid hyperplasia in the SENCAR mouse: Differentiation from granulocytic leukemia. Environ Health Perspect. 1986; 68:117–123. [PubMed: 3465532]

Mahler JF, Flagler ND, Malarkey DE, Mann PC, Haseman JK, Eastin W. Spontaneous and chemically induced proliferative lesions in Tg.AC transgenic and p53-heterozygous mice. Toxicol Pathol. 1998; 26:501–511. [PubMed: 9715509]

Markivits JE, Sahota PS. Granular cell lesions in the distal female reproductive tract of aged Sprague Dawley rats. Vet Pathol. 2000; 37:439–448. [PubMed: 11055867]

Maronpot RR, Montgomery CA, Boorman GA, McConnell EE. National Toxicology Program nomenclature for hepatoproliferative lesions of rats. Toxicol Pathol. 1986; 14:163–273.

Mitsumori K, Maronpot RR, Boorman GA. Spontaneous tumors of the meninges in rats. Vet Pathol. 1987; 24:50–58. [PubMed: 3824823]

Mohr, U., editor. Fascicle No. 7: Central Nervous System, Heart, Eye, Mesothelium. Vol. No. 122. Lyon, France: IARC Scientific Publications; 1994. International Classification of Rodent Tumours, Part I, The Rat; p. 1-33.

Morgan KT, Frith CH, Swenberg JA, McGrath JT, Zulch KJ, Crowder DM. A morphologic classification of brain tumors found in several strains of mice. J Natl Cancer Inst. 1984; 72:151–160. [PubMed: 6582295]

Narama I, Imaida K, Iwata H, Nakae D, Nishikawa A, Harada T. A review of nomenclature and diagnostic criteria for proliferative lesions in the liver of rats by a working group of the Japanese Society of Toxicologic Pathology. Toxicol Pathol. 2003; 16:1–17.

[accessed August 27, 2009] National Toxicology Program Historical Control Database. http://ntp-server.niehs.nih.gov

Solleveld, HA.; Boorman, GA. Brain. In: Boorman, GA.; Eustis, SL.; Elwell, MR.; Montgomery, CA.; MacKenzie, WF., editors. In Pathology of the Fischer Rat: Reference and Atlas. San Diego, California: Academic Press, Inc; 1990. p. 168-170.

Solleveld, HA.; Gorgacz, EJ.; Koestner, A. In Standardized System of Nomenclature and Diagnostic Criteria: Guides for Toxicologic Pathology. Washington, DC: STP/ ARP/AFIP; 1991. Central nervous system neoplasms in the rat; p. 1-17.

Squire RA, Levitt MH. Report of a workshop on classification of specific hepatocellular lesions in rats. Cancer Res. 1975; 35:3214–3223. [PubMed: 171067]

Stewart HL, Williams G, Keysser CH, Lombard LS, Montali RJ. Histologic typing of liver tumors of the rat. J Natl Cancer Inst. 1980; 64:177–206. [PubMed: 6986002]

Trempus CS, Ward S, Farris G, Malarkey D, Faircloth RS, Cannon RE, Mahler JF. Association of v-Ha-ras transgene expression with development of erythroleukemia in Tg.AC transgenic mice. Am J Pathol. 1998; 153:247–254. [PubMed: 9665485]

Turusov VS, Torii M, Sill RC, Willson GA, Herbert RA, Hailey JR, Haseman JK, Boorman GA. Hepatoblastomas in mice in the US National Toxicology Program (NTP) studies. Toxicol Pathol. 2002; 30:580–591. [PubMed: 12371667]

Vahle J, Bradley A, Harada T, Herbert R, Kaufmann W, Kellner R, Mann P, Pyrah I, Rittinghausen S, Tanaka T. The international nomenclature project: An update. Toxicol Pathol. 2009; 37:694–697. [PubMed: 19638442]

Yoshida T, Mitsumori K, Harada T, Maita K. Morphological and ultrastructural study of the histogenesis of meningeal granular cell tumors in rats. Toxicol Pathol. 1997; 25:211–216. [PubMed: 9125780]

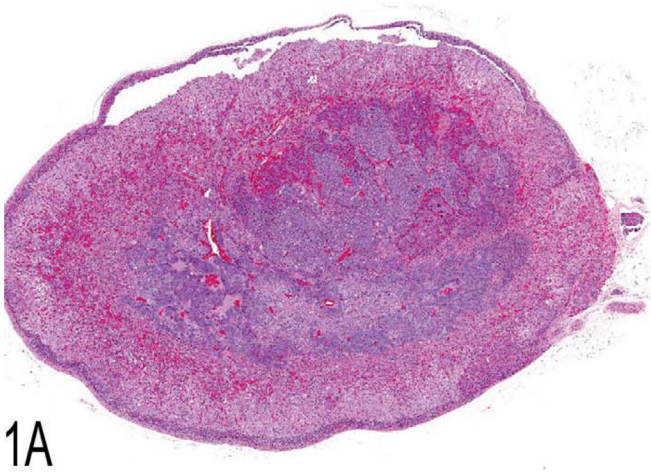

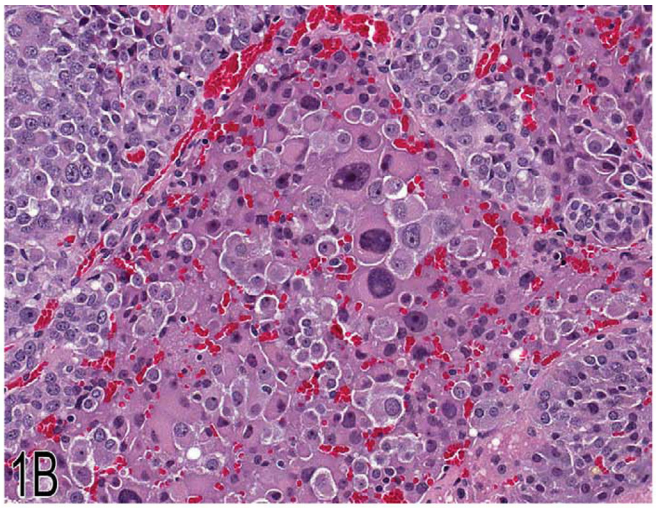

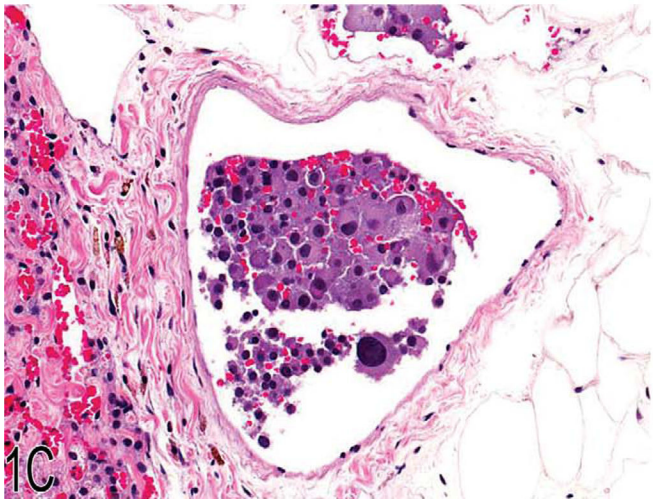

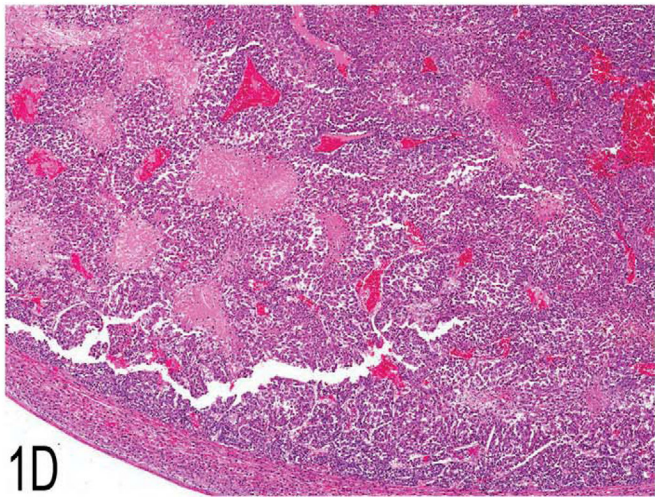

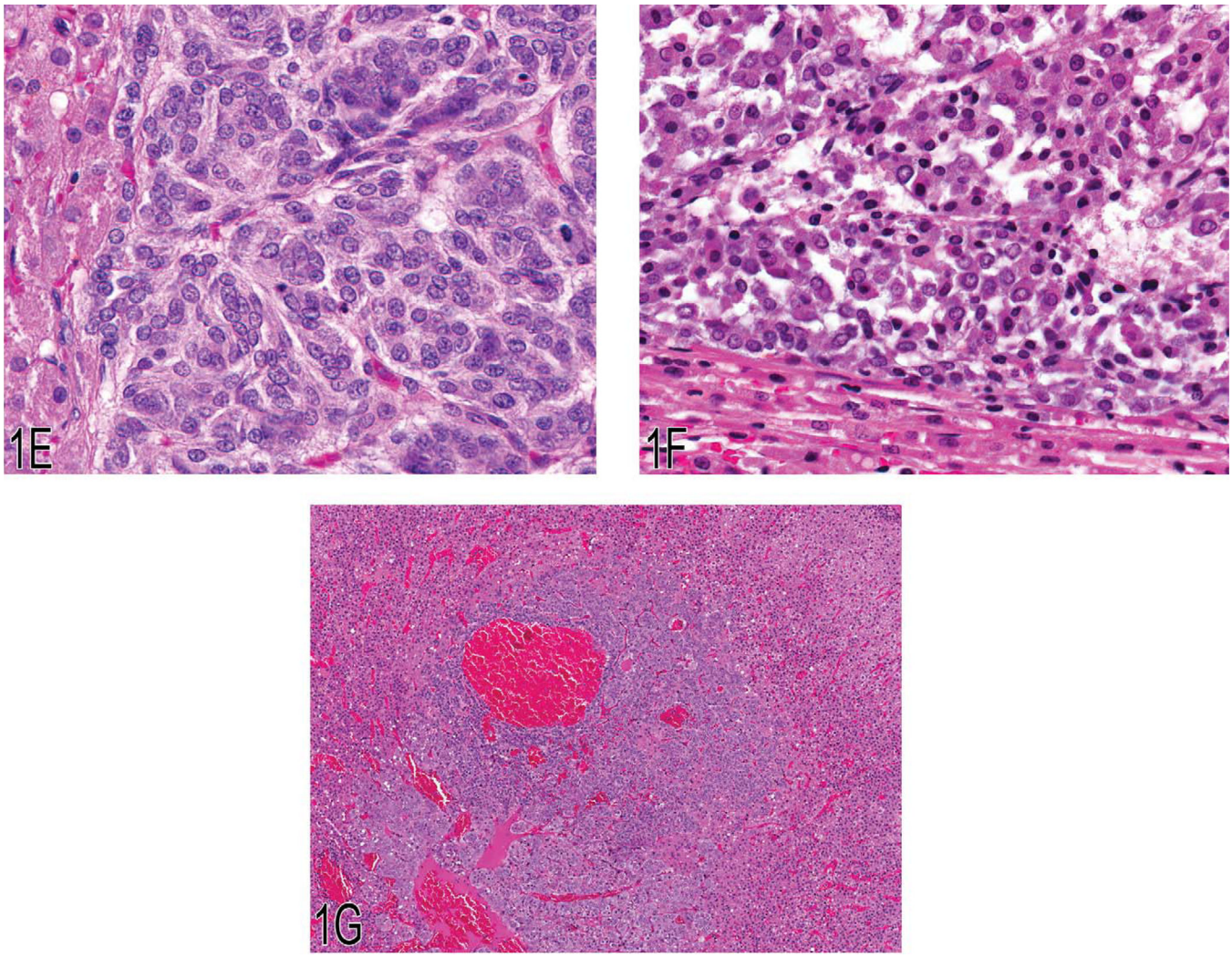

Figure 1.

(A) Malignant pheochromocytoma with neoplastic cells in the periadrenal vasculature. (B) Pleomorphic neoplastic cells from the malignant pheochromocytoma shown in (A). (C) Neoplastic cells in the lumen of a periadrenal blood vessel from the malignant pheochromocy-toma shown in (A). (D) Compressive adrenal medullary mass with necrosis. (E) Cellular features of an adrenal medullary neuroblastoma. Note the closely packed neoplastic neuroblasts with scant cytoplasm. (F) Cellular features of the malignant pheochromocytoma shown in (D). Note the sheet of neoplastic chromaffin cells with abundant cytoplasm. (G) Focal hyperplasia of the adrenal medulla.

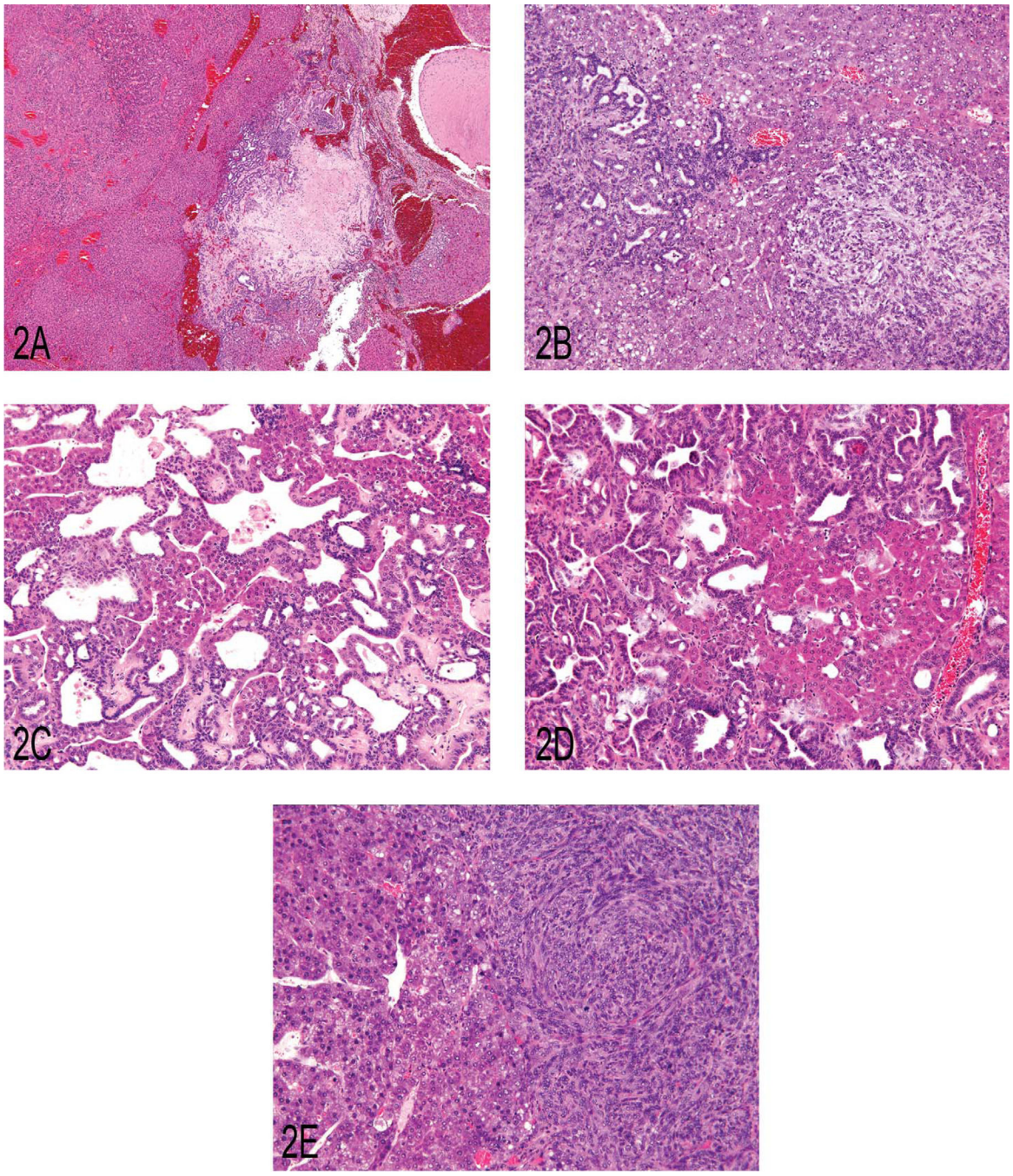

Figure 2.

(A) Primary liver neoplasm demonstrating the classic presentation of a hepatocholangiocarcinoma (HCCC) as seen in the B6C3F1 mouse. There is an area of malignant hepatocellular proliferation (arrow) and areas of malignant ductal cell proliferation (arrowhead) adjacent to an area of necrosis and near an area of a cystlike formation (asterisk). (B) A portion of a primary HCCC demonstrating an area of malignant duct proliferation (arrow) and a focus of undifferentiated malignant cell proliferation (arrowhead) in a bed of hepatocellular carcinoma. (C) A primary HCCC demonstrating

cords of hepatocellular carcinoma transitioning/blending into malignant cuboidal and columnar epithelium, forming ducts of varying morphological character. (D) A metastatic lesion of an HCCC as seen in the lung. Note the presence of malignant hepatocytes and duct-forming epithelial cells. (E) An HCCC that metastasized to the lung that demonstrates malignant hepatocyte proliferation and adjacent proliferation of an undifferentiated cell type.

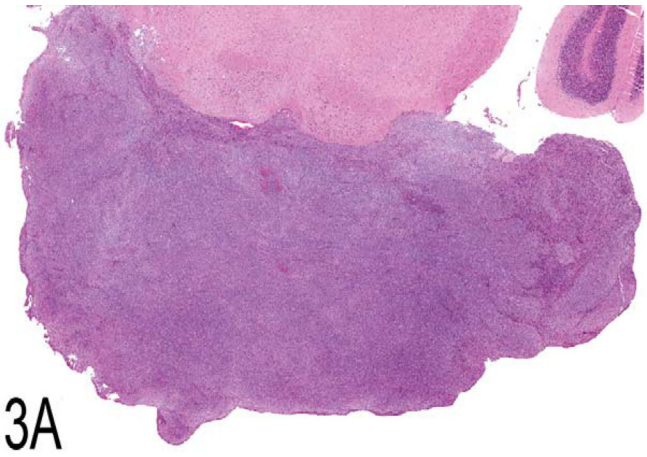

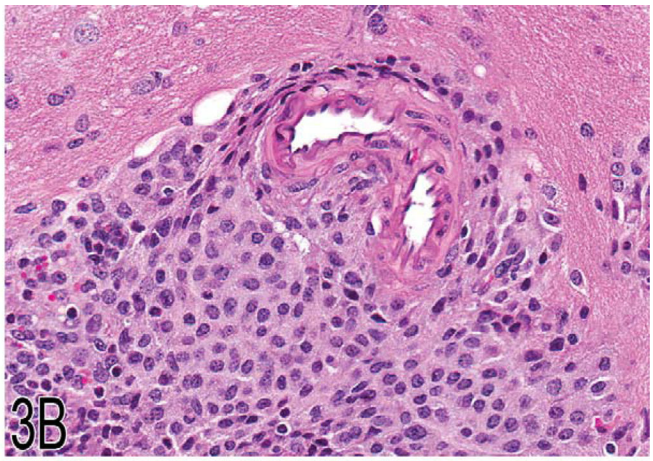

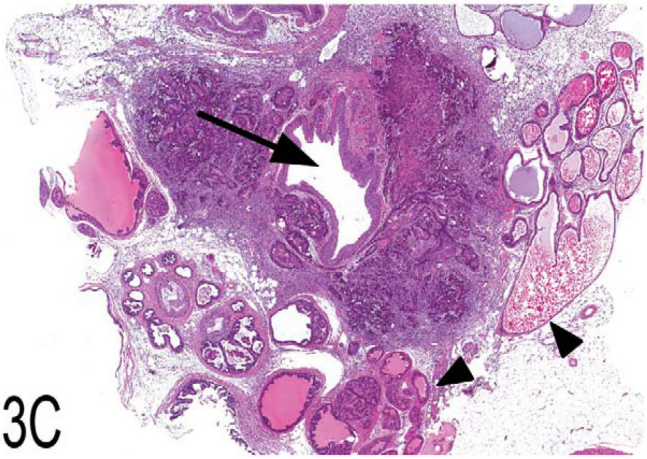

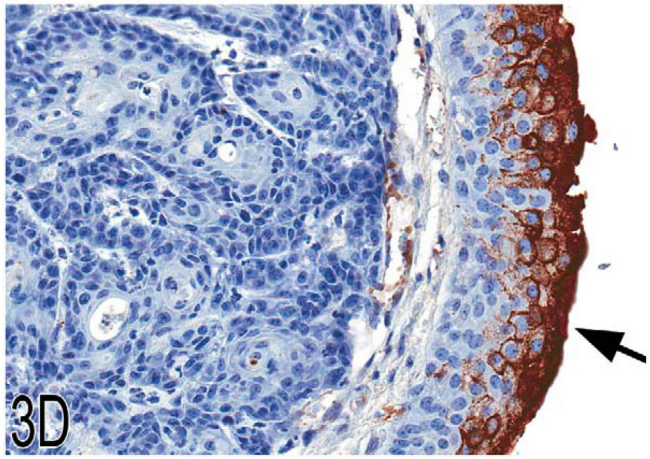

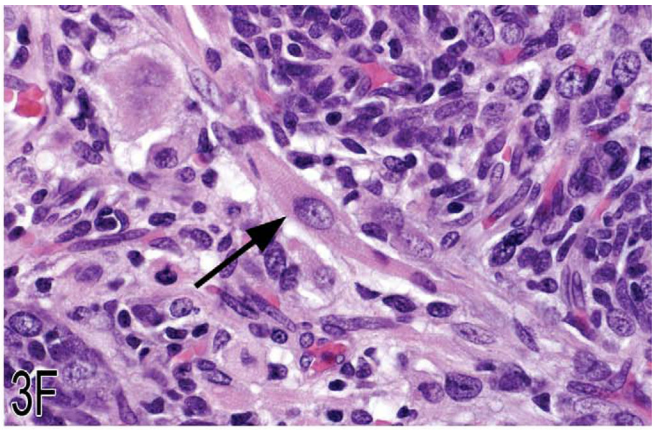

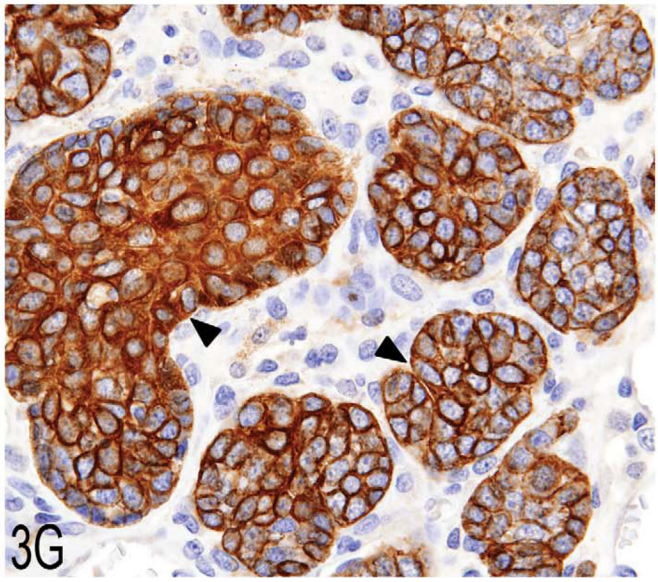

Figure 3.

(A, B) Low and high magnifications of a histiocytic sarcoma located in the brain of a B6C3F1 mouse. (C, D) Low and high magnification of a urethral transitional cell carcinoma arising from the proximal urethra (arrow) and invading into adjacent tissues, including the secondary sex glands (arrowheads). Hematoxylin and eosin (C) and uroplakin III immunohistochemistry (D). (E–G) Gross image of a thymoma (E) from the anterior mediastinum of a 1.5-year-old female F344 rat and high magnification illustrating the presence of an occasional large myoid cell (arrow) with abundant eosinophilic and granular cytoplasm and striations. Immunohisto-chemically, epithelial nests are strongly positive for cytokeratin (arrowheads), consistent with epithelial components of a thymoma.

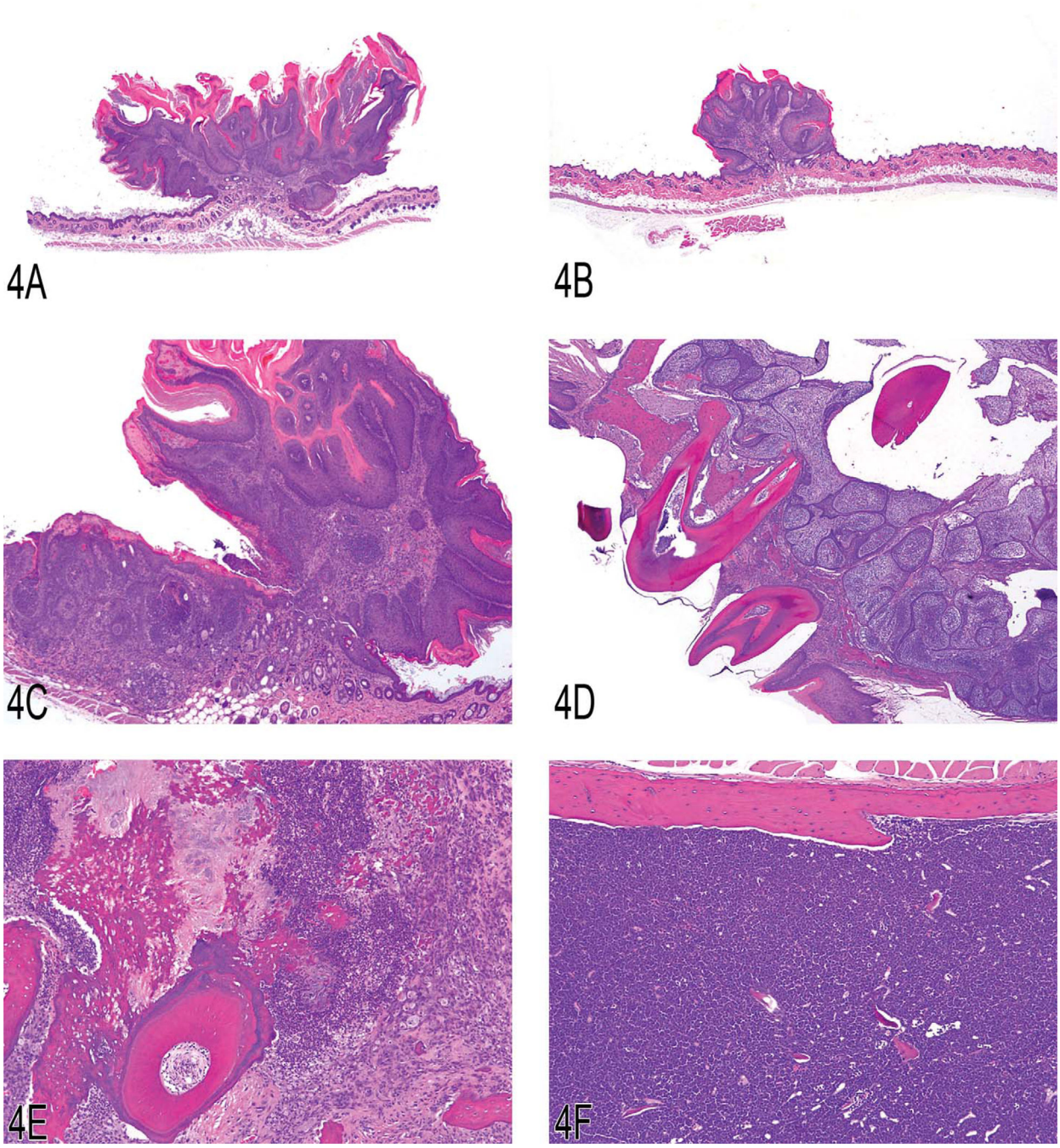

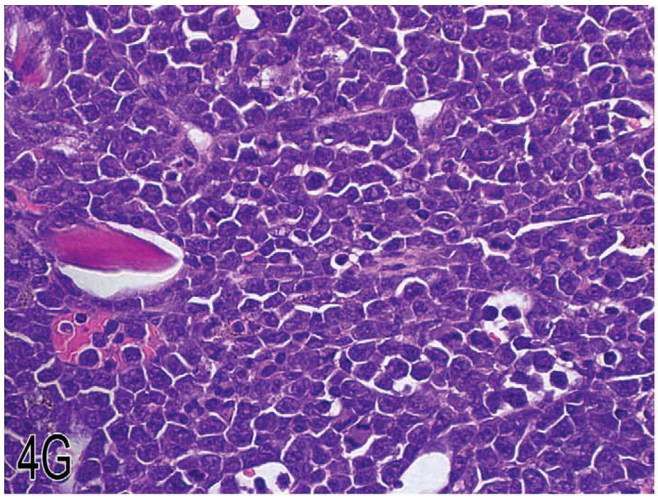

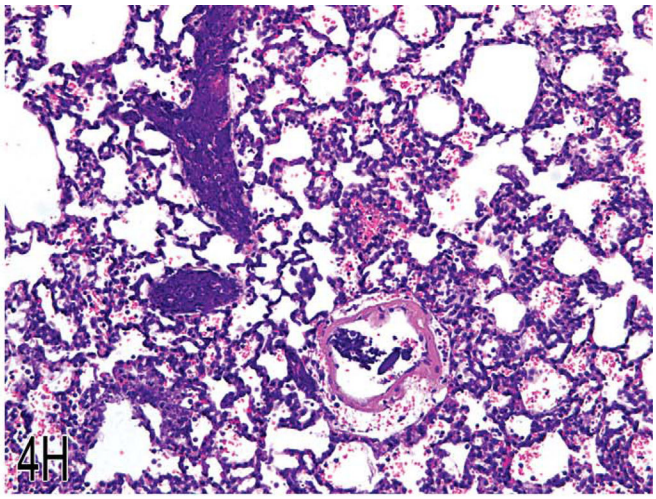

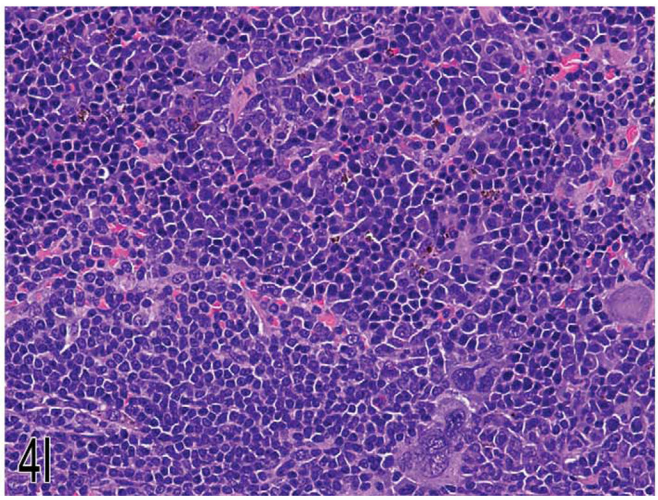

Figure 4.

(A) Typical skin lesion from a Tg.AC mouse (squamous papilloma). (B) Skin lesion from a Tg.AC mouse (squamous papilloma). (C) Malignant squamous cell transformation adjacent to a papilloma in a Tg.AC mouse. (D) Odontoma with tooth elements from a Tg.AC mouse. (E) Atypical odontoma from the oral cavity of a Tg.AC mouse. (F) Erythroleukemia in the bone marrow of a Tg.AC mouse. (G) Erythroleukemia in the bone marrow of a Tg.AC mouse (higher magnification). (H) Erythroleukemia in the lung of a Tg.AC mouse. Pulmonary capillaries are highly cellular. (I) Splenic extramedullary hematopoiesis in a Tg.AC mouse. Megakaryocytic, myeloid, and erythroid cells are present within the hypercellular splenic parenchyma.

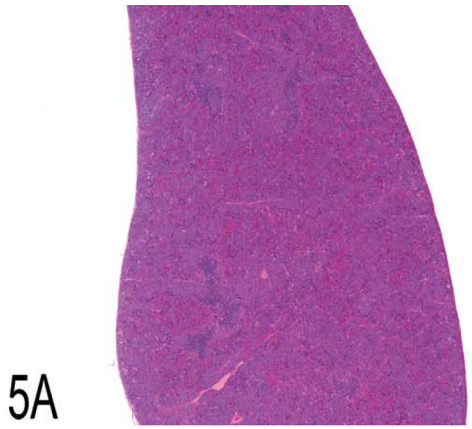

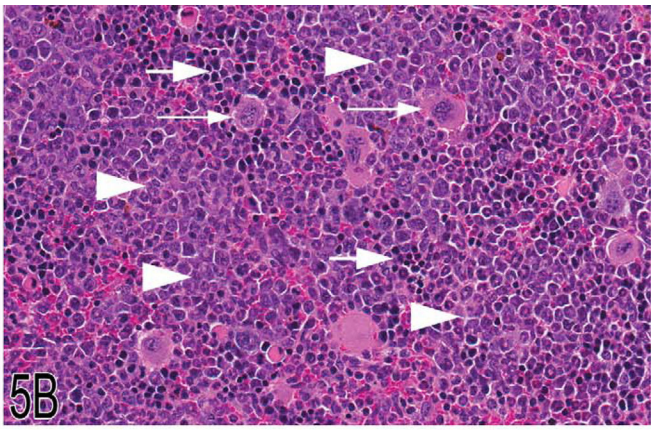

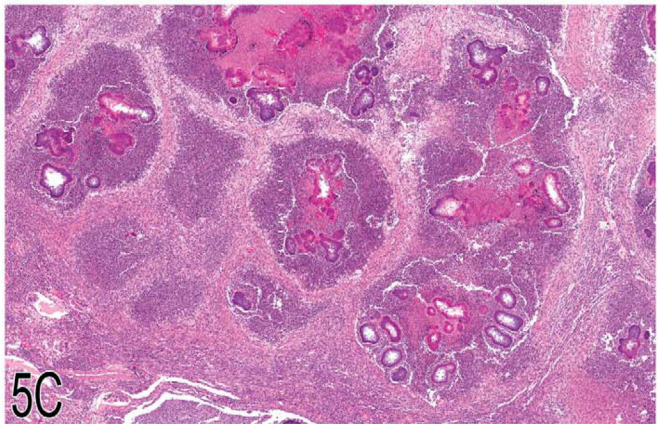

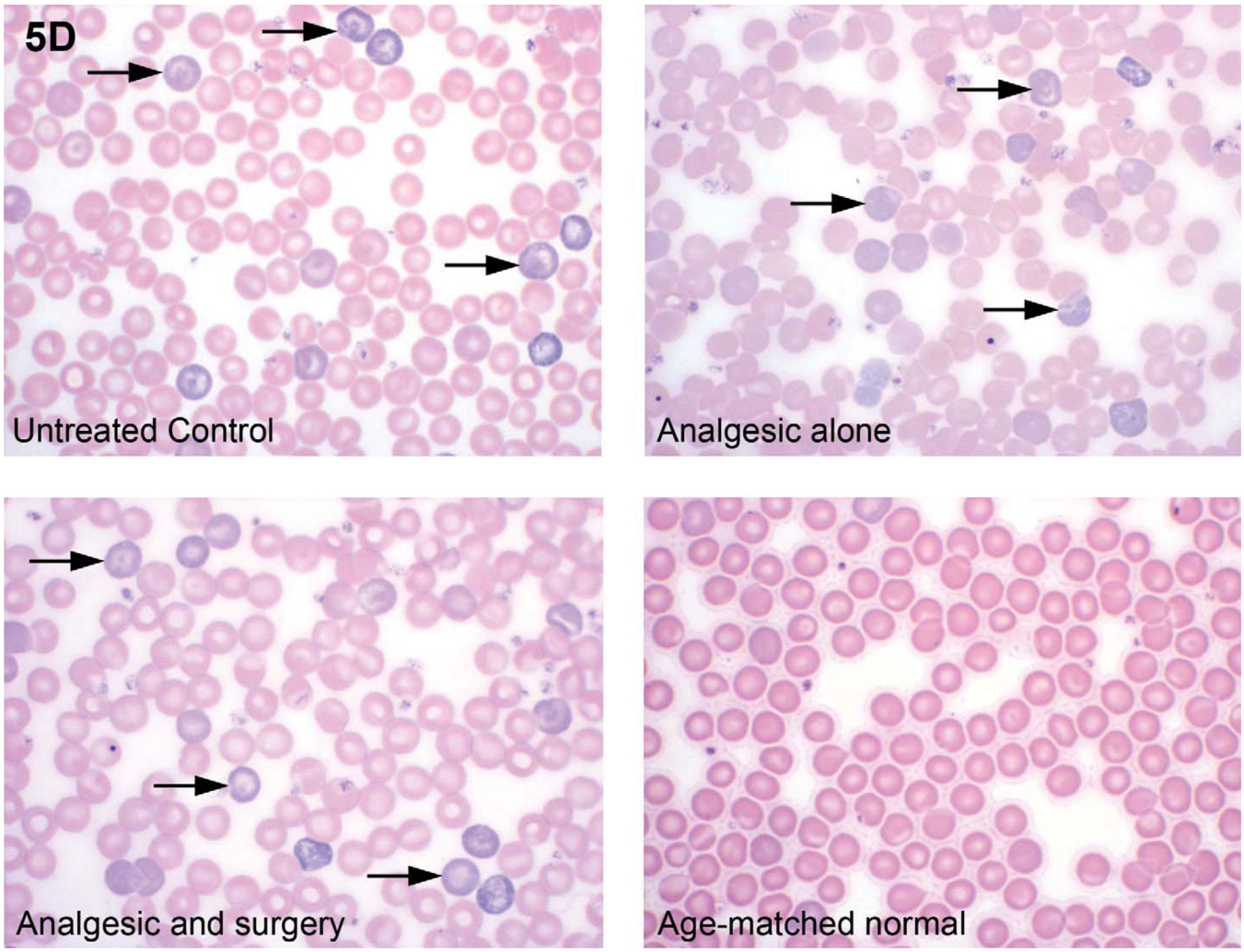

Figure 5.

(A, B) Spleen from a 1.5-year-old female C57BL/6NCrl mouse with a marked degree of hematopoietic cell proliferation. There is expansion of the red pulp by large numbers of hematopoietic cells, resulting in effacement of the white pulp (A). High magnification of this excessive splenic hematopoietic cell proliferation (B) demonstrates a predominance of myeloid cells in various stages of development (arrowheads), as well as erythroid cells (large arrows) and numerous megakaryocytes (small arrows). (C) Low magnification of the liver from the female mouse presented in (A) and (B) demonstrating a severe, multifocal to coalescing, pyogranulomatous hepatitis with intralesional Splendore-Hoeppli material and bacterial colonies. (D) Mouse blood smears demonstrating an increased number of polychromatophilic erythrocytes (arrows) in animals from a four-day study evaluating the effect of analgesia on postsurgical recovery (untreated control, analgesic alone, analgesic and surgery). This blood was collected four days postsurgery. However, these animals also had two previous blood collections (three days prior to surgery and one day postsurgery) prior to collection of blood for the final smear and CBC at day four post surgery. For comparison, the fourth image is that of an age-matched normal animal that was not part of the study (Romanowsky).

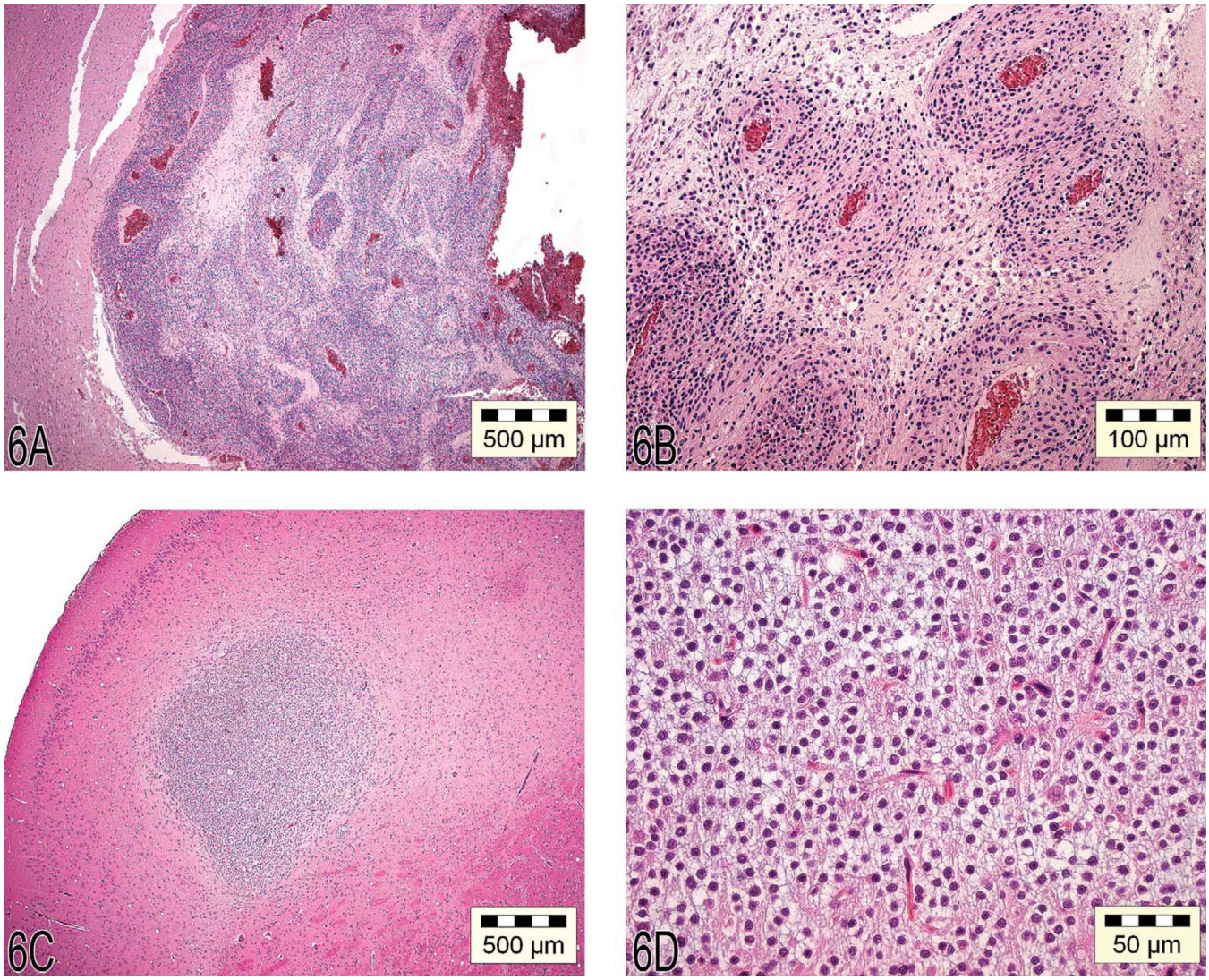

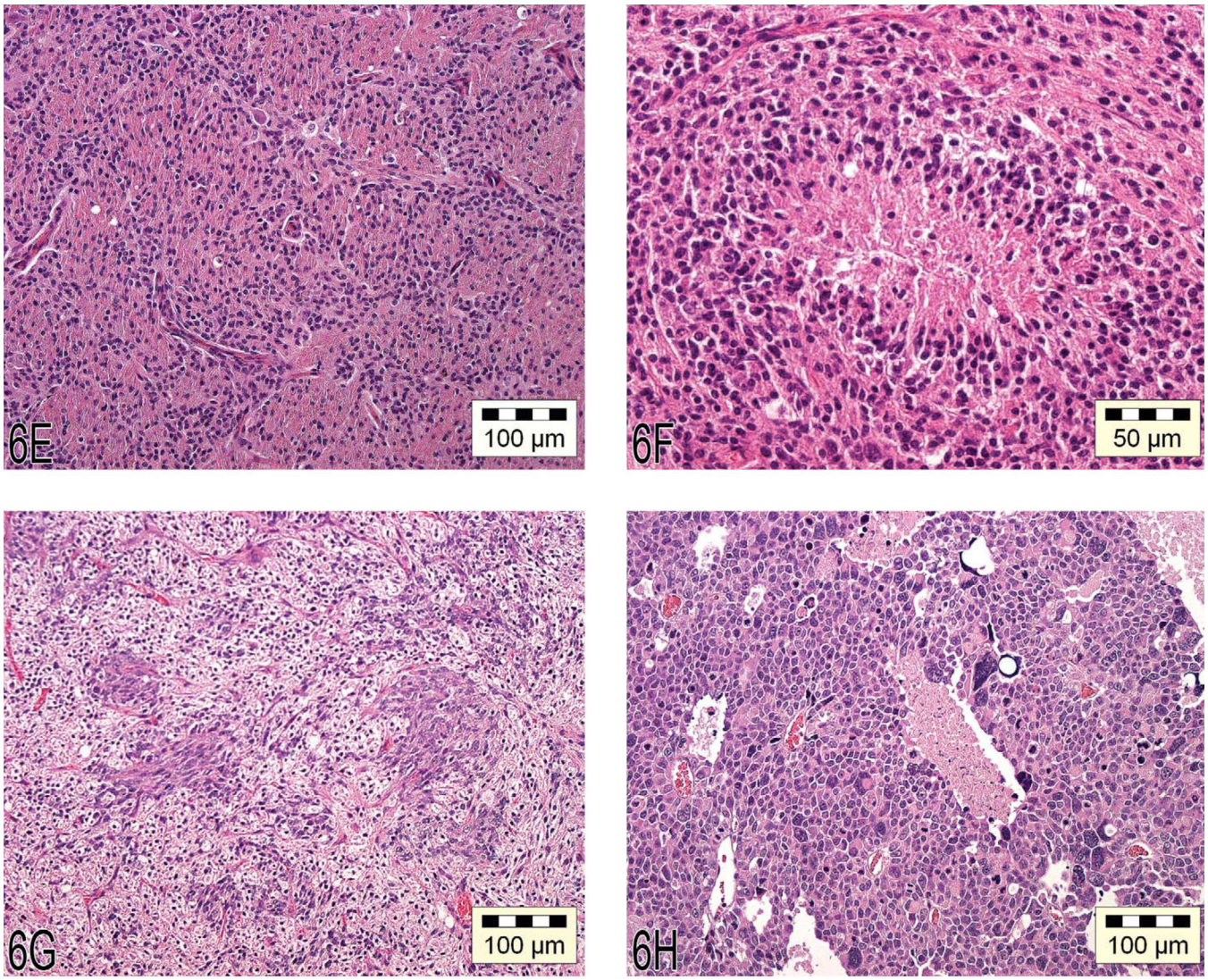

Figure 6.

(A) “Malignant” oligodendroglioma characterized by large, well-circumscribed lesions spread over multiple areas of the brain, with necrosis and hemorrhage. (B) Atypical capillary endothelial hyperplasia characteristic of malignant oligodendrogliomas. (C) “Benign” oligoden-droglioma characterized by a small, well-circumscribed lesion that is confined to one major area of the brain. (D) The benign oligodendroglioma often shows a “honeycomb” or “fried egg” cell pattern. (E) Astrocytoma with cells that have protoplasmic or fibrillary differentiation and prominent round or oval nuclei. (F) Necrosis with pseudopalisading is one characteristic feature of astrocytomas. (G) The mixed glioma of the mouse can show both proliferative astrocytoma and oligodendroglioma-like features. (H) A malignant pinealoma often expands by invasion into the adjacent brain tissue and is highly cellular, rich in mitotic figures, and pleomorphic.

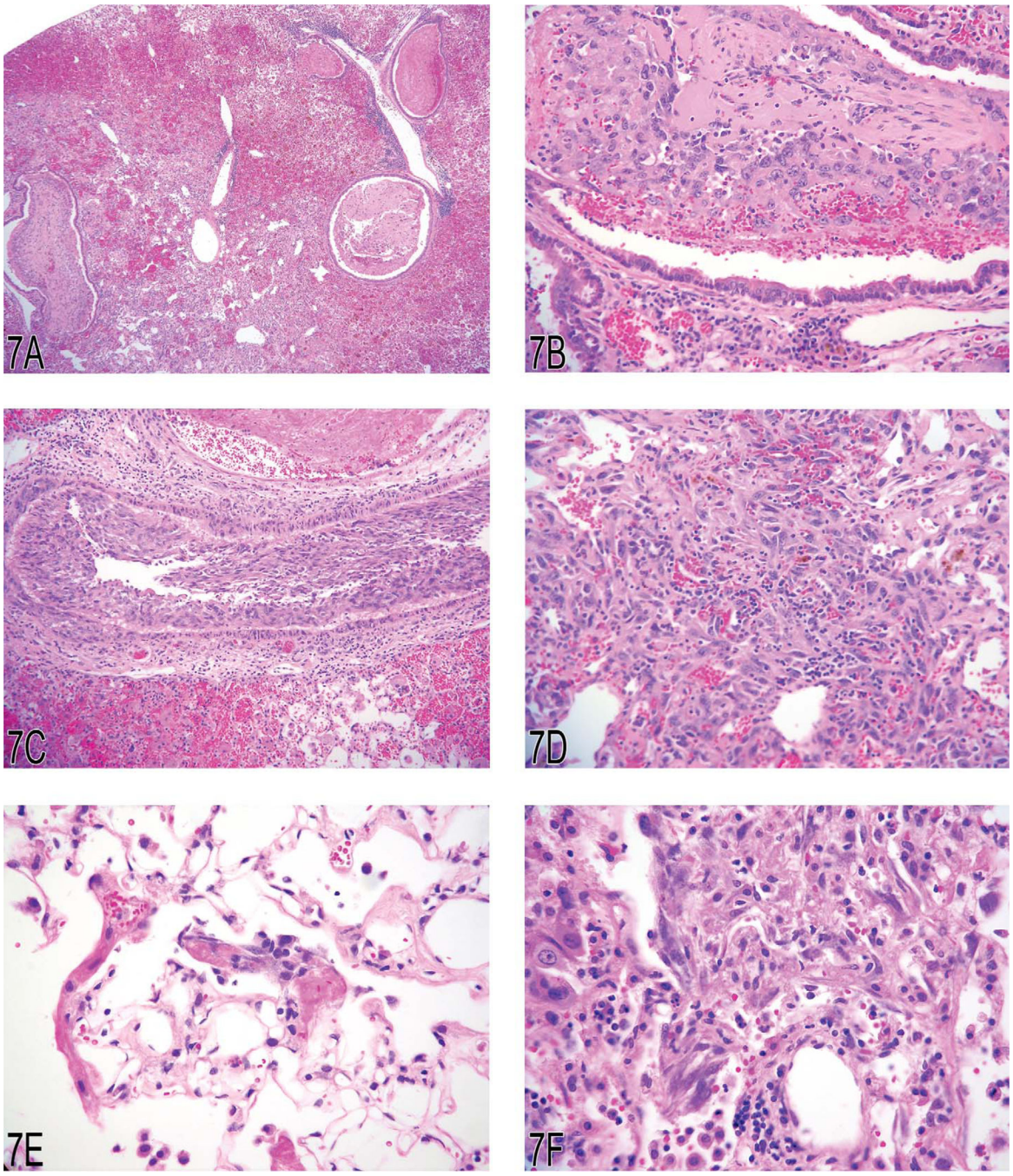

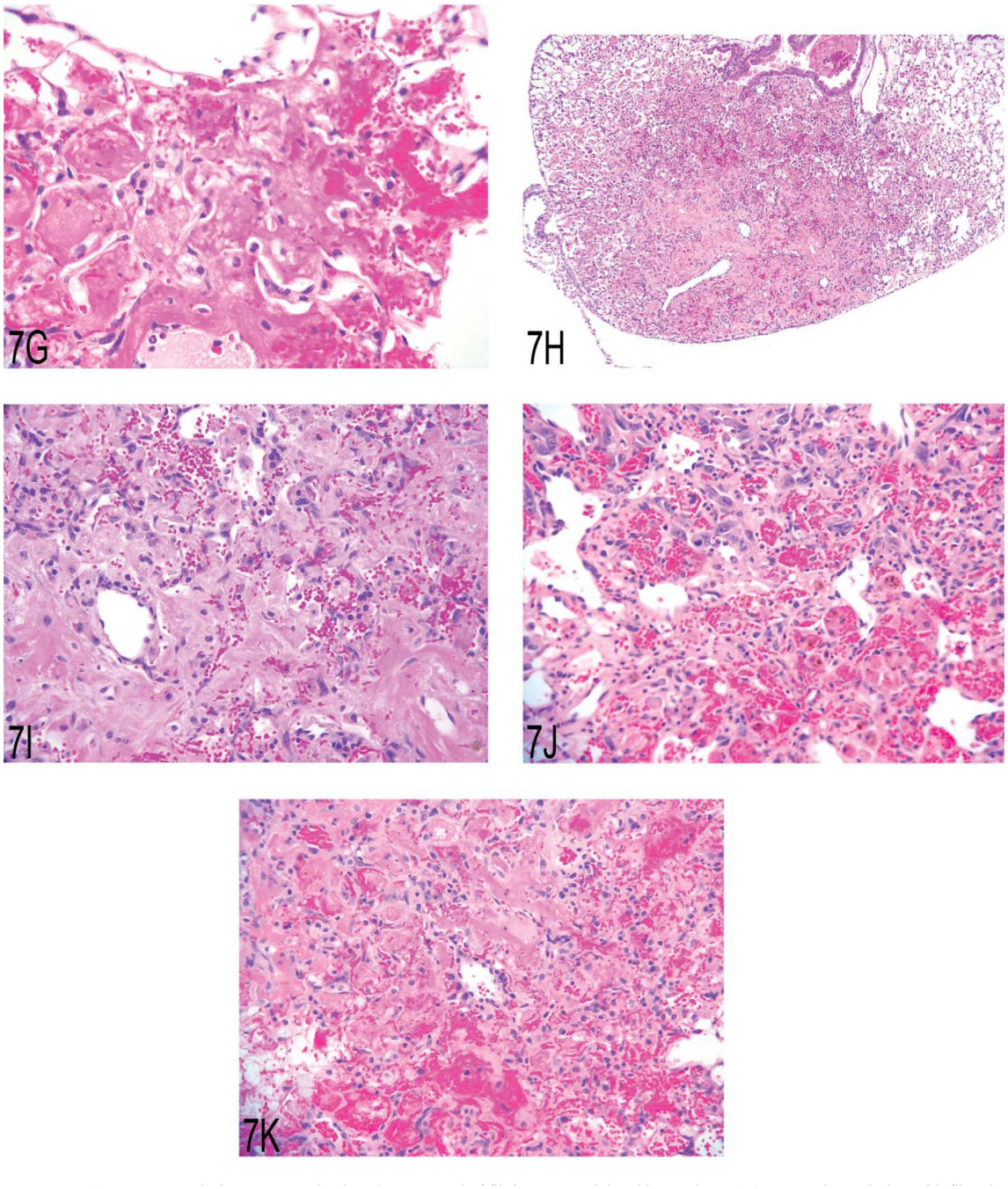

Figure 7.

(A) Lung: hemangiosarcoma with hemorrhage and hemosiderin. (B) Lung, airway: organized fibrinous material and ingrowth of neoplastic endothelial cells. (C) Lung, vessel: neoplastic endothelial cells. (D) Lung: hemangiosarcoma. (E) Lung: small (possibly early) lesion with fibrinous material, fibrosis, and hypertrophic spindle (endothelial?) cells. (F) Lung: changes similar to those in 7E are present in this slightly larger lesion. (G) Lung: some lesions were predominately composed of fibrinous material and hemorrhage. (H) Lung: a larger lesion with fibrosis, hemorrhage, and hemosiderin. (I) Lung: higher

magnification of (H). (J) Lung: the morphology of the bottom portion of this lesion looks similar to (I); however, there is unequivocal neoplastic transformation noted in the upper portion. (K) Lung: this lesion was diagnosed as angiomatous hyperplasia/fibrosis in the study, but there was no consensus from the audience.

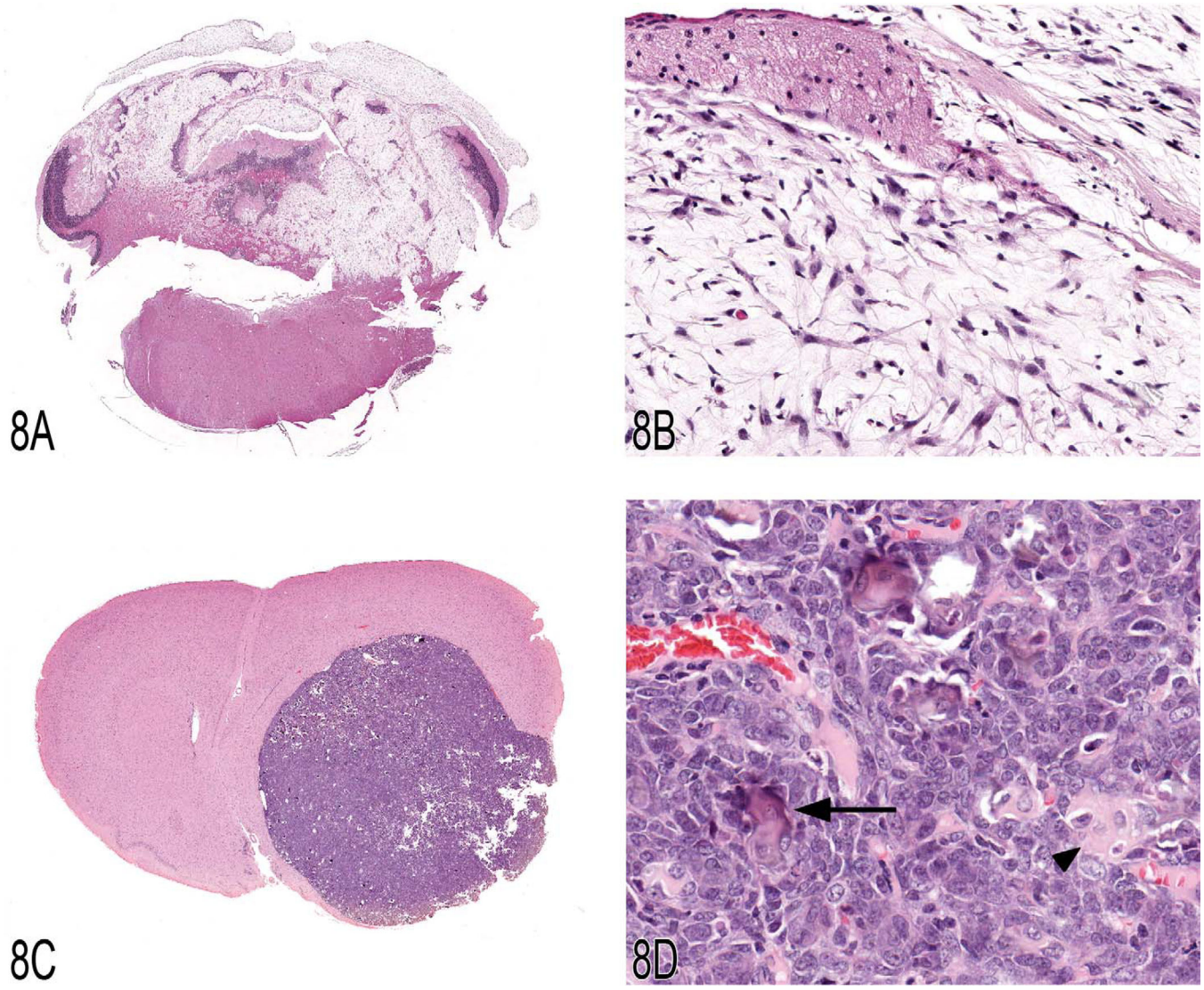

Figure 8.

(A, B) B6C3F1 mouse, cerebellum, low and high magnification, respectively. The cerebellum is invaded and destroyed by a paucicellular meningeal neoplasm composed of spindle to stellate-shaped cells surrounded by a myxoid matrix (myxoid malignant meningioma). (C, D) Fischer 344 rat, forebrain, low and high magnification, respectively. The forebrain is markedly compressed by a well-circumscribed mass composed of small lobules frequently containing small foci of hyalinized collagen and mineralization consistent with psammoma bodies (psammomatous meningioma).

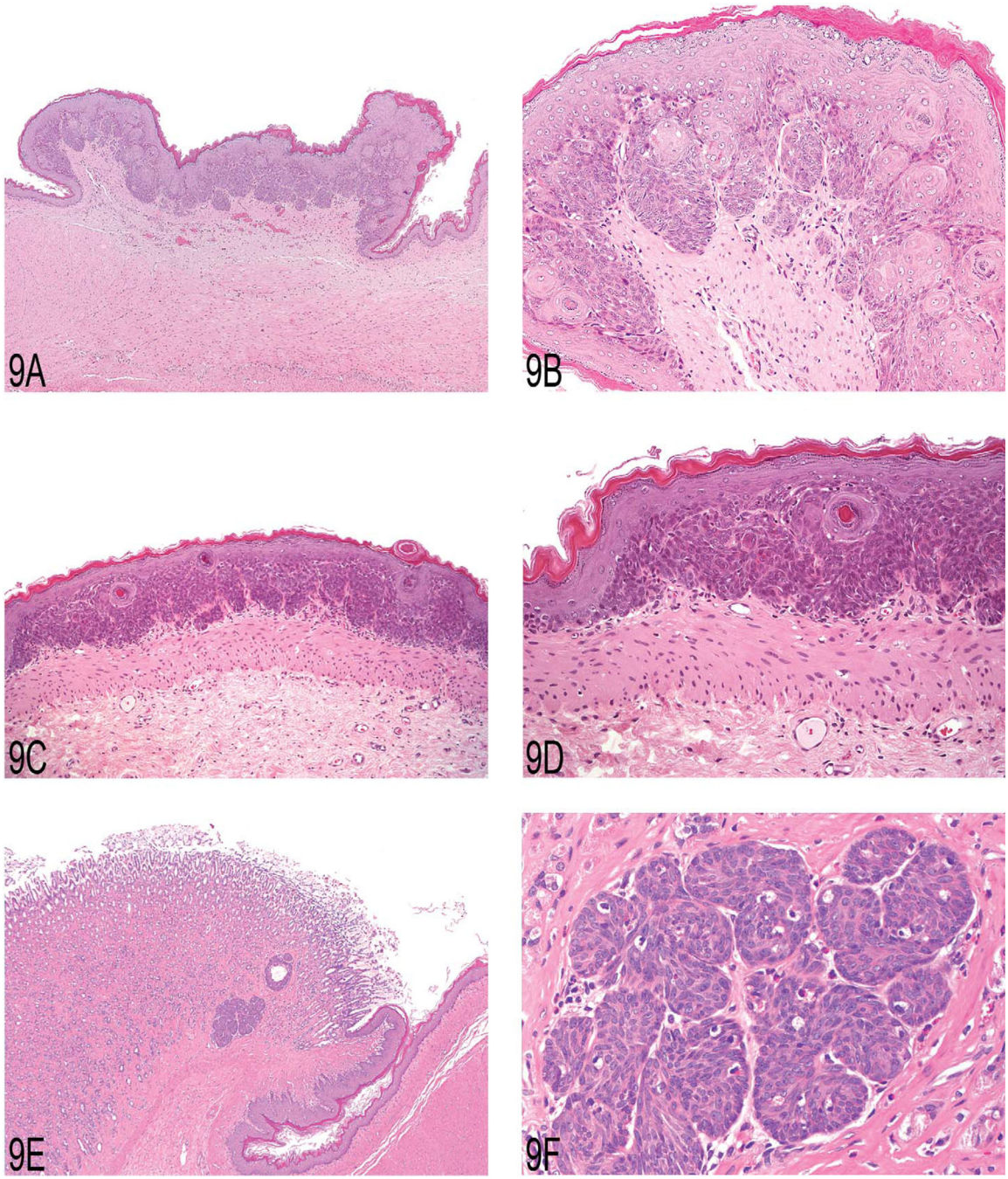

Figure 9.

(A) Focal epithelial proliferation in the forestomach of a two-year-old female Wistar rat. Note elevation from the adjacent unaffected epithelium mimicking a “sessile papilloma.” (B) Higher magnification showing prominent development of rete pegs, built up mainly by basal and prickle cells. (C) Focal basal cell hyperplasia in the forestomach of a two-year-old female Wistar rat. Note proliferation of basal cell layers and orderly structure of stratum granulosum and corneum. (D) Higher magnification of (C) showing proliferation of basal cells forming tightly packed papillary projections. (E) Proliferation of basal cells in the

gastric glandular mucosa of a two-year-old male Wistar rat. Note proximity to the limiting ridge. (F) Higher magnification of (E) demonstrating the basal cell character of this epithelial proliferation.

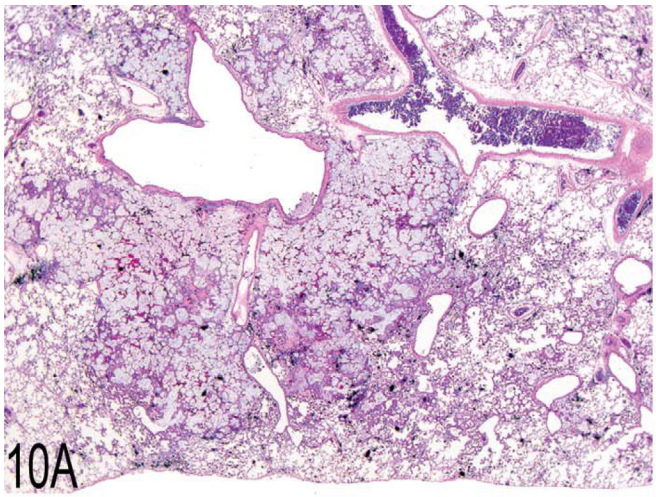

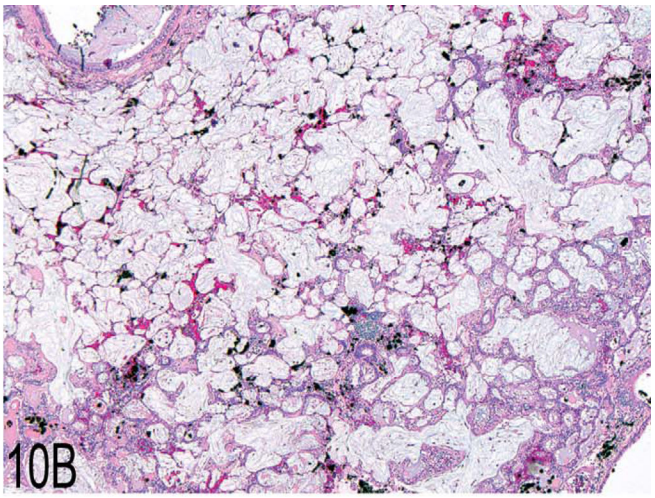

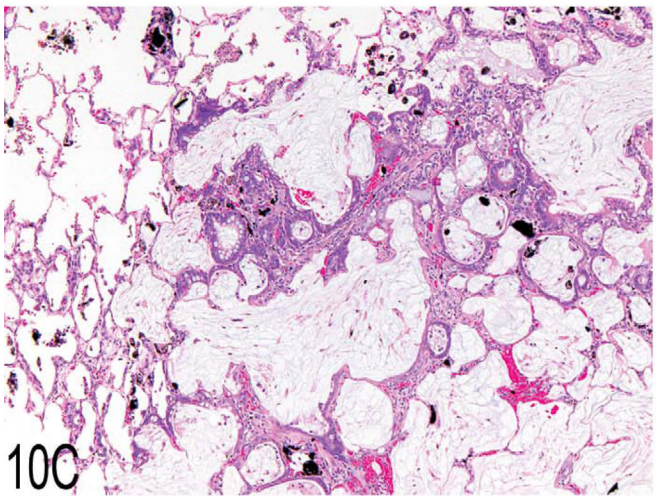

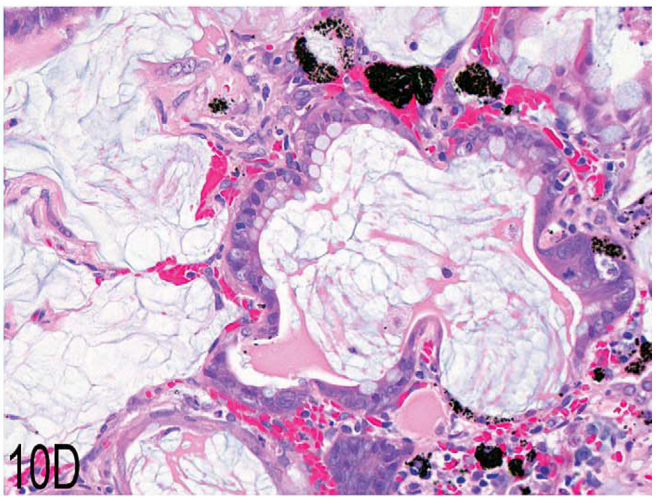

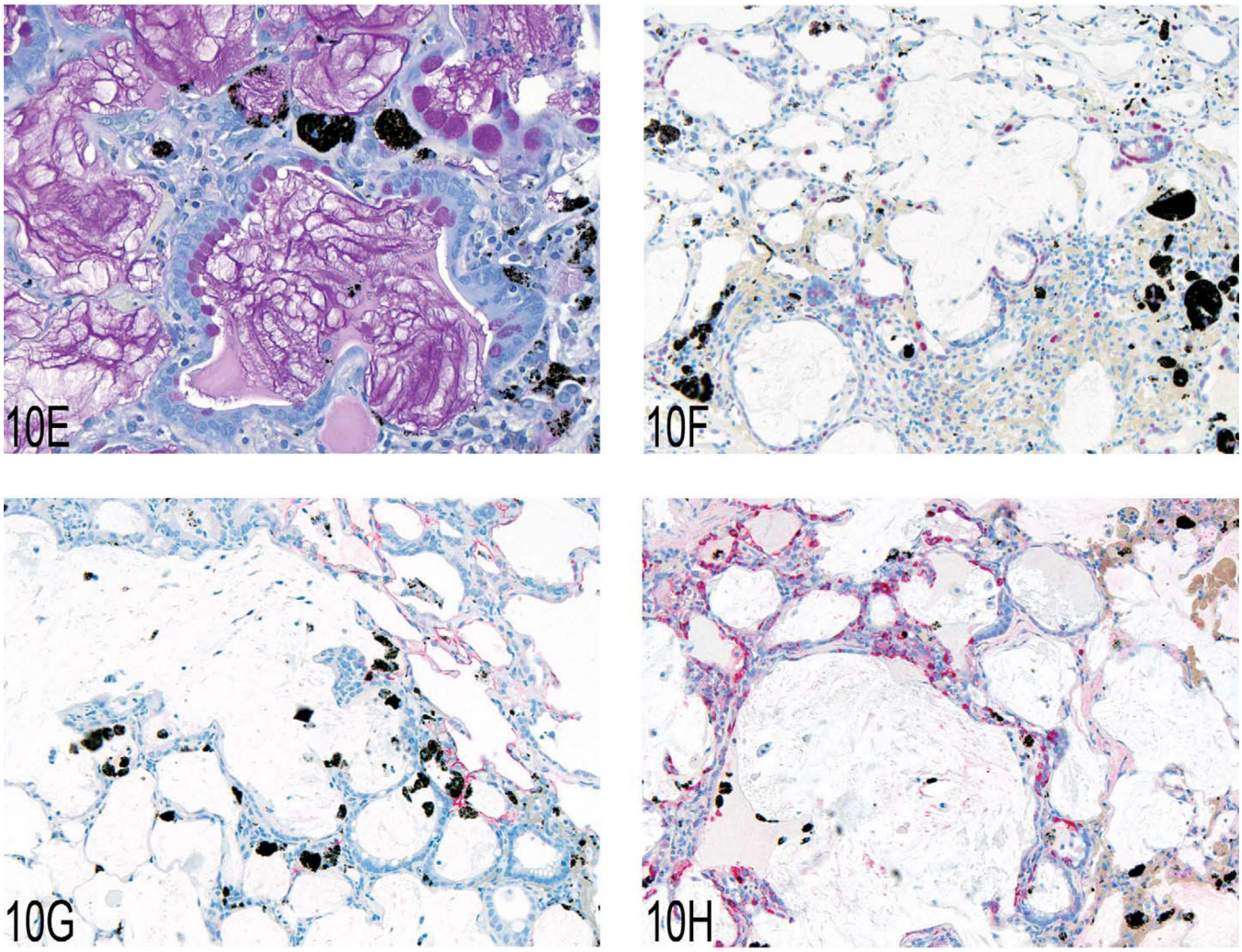

Figure 10.

(A–D) Pulmonary mucous cell metaplasia in rat lung after intratracheal instillation of diesel engine exhaust. Hematoxylin and eosin. (E) Periodic acid Schiff–positive material within the lesions of exaggerated mucous cell metaplasia. (F) Immunohistochemistry using anti-PCNA and chromogen Fast Red showing proliferating epithelial and inflammatory cells and black pigment from diesel engine exhaust. (G) Immunohistochemistry using anti-CD54 (ICAM-1) and chromogen Fast Red with positive staining of alveolar type I and type II cells in the lung tissue adjacent to the lesion. (H) Immunohistochemistry using anti-Clara cell secretory protein and chromogen Fast Red illustrating the location and number of Clara cells within the treated lung.

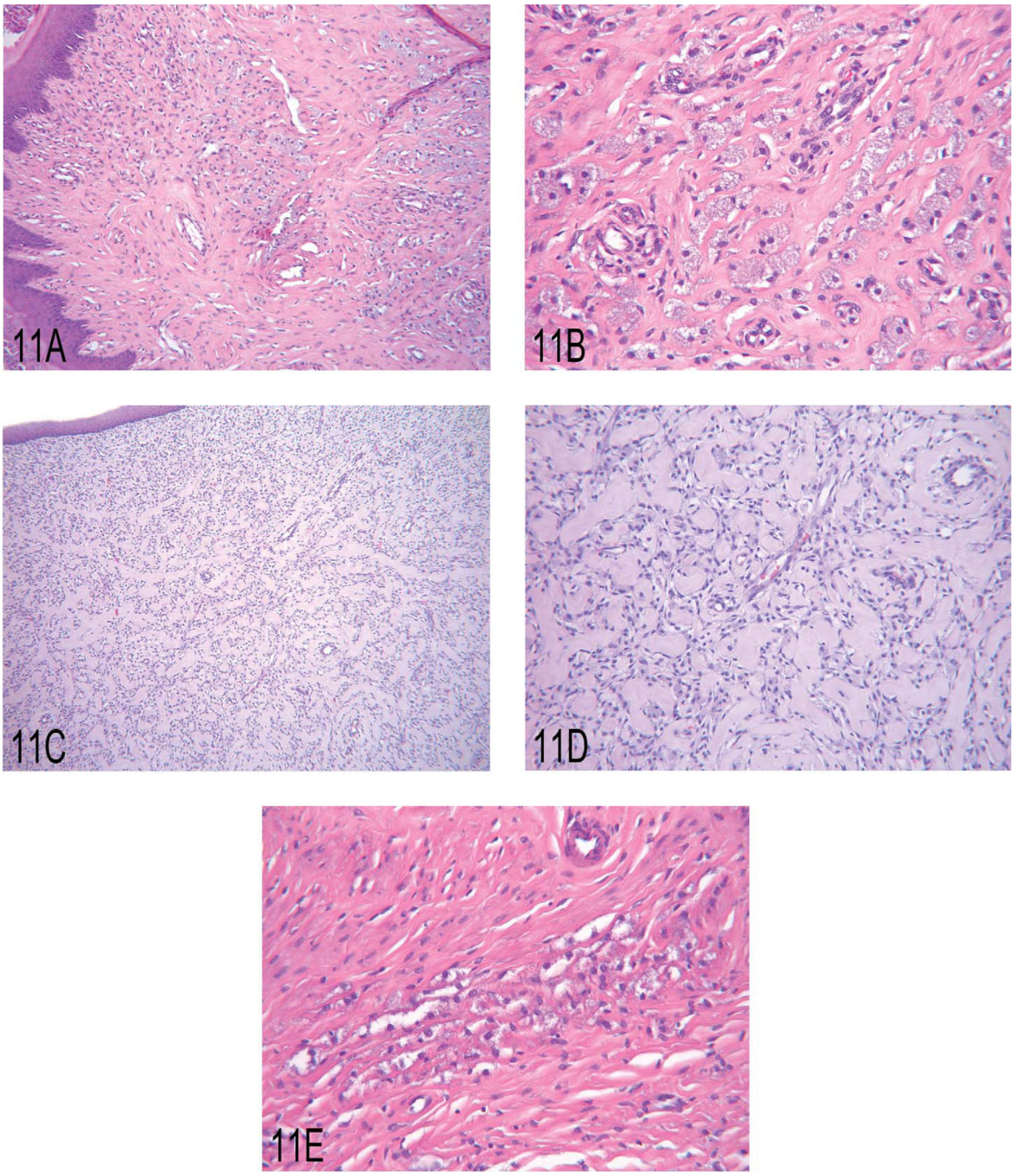

Figure 11.

(A, B) Low and high magnification, respectively, of granular cell hyperplasia in the uterine cervix of a rat. (C, D) Low and high magnification, respectively, of a benign granular cell tumor in the uterine cervix of a rat. (E) Granular cell aggregate in the uterus of a rat.

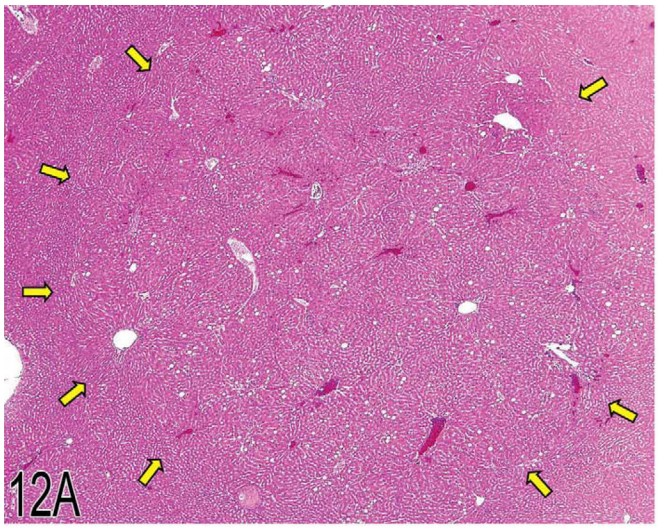

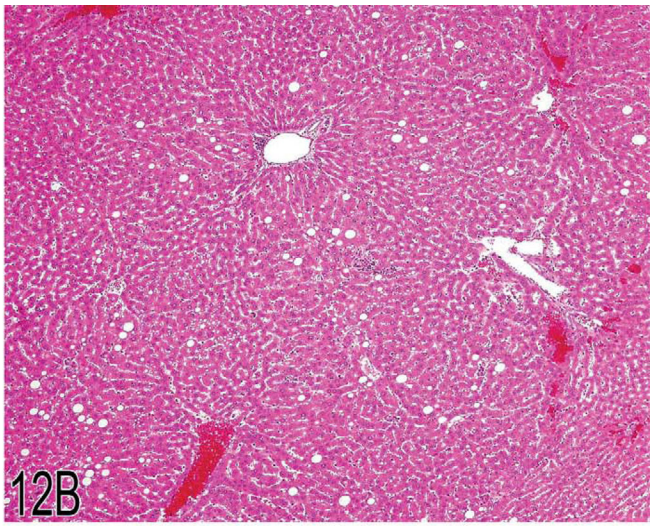

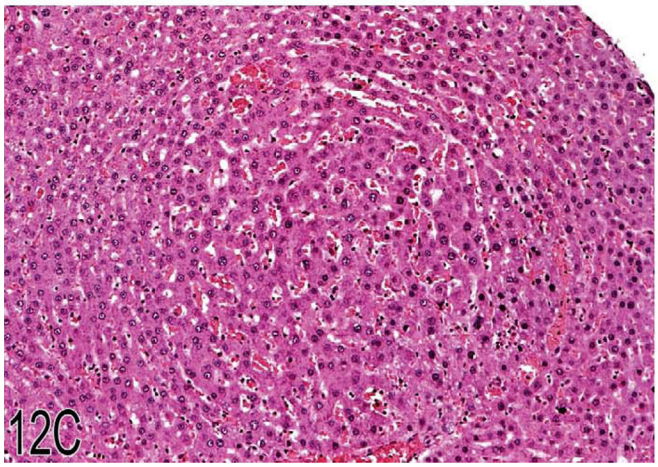

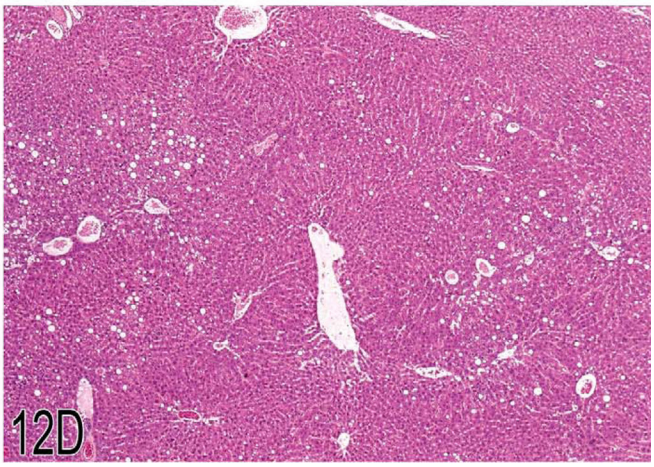

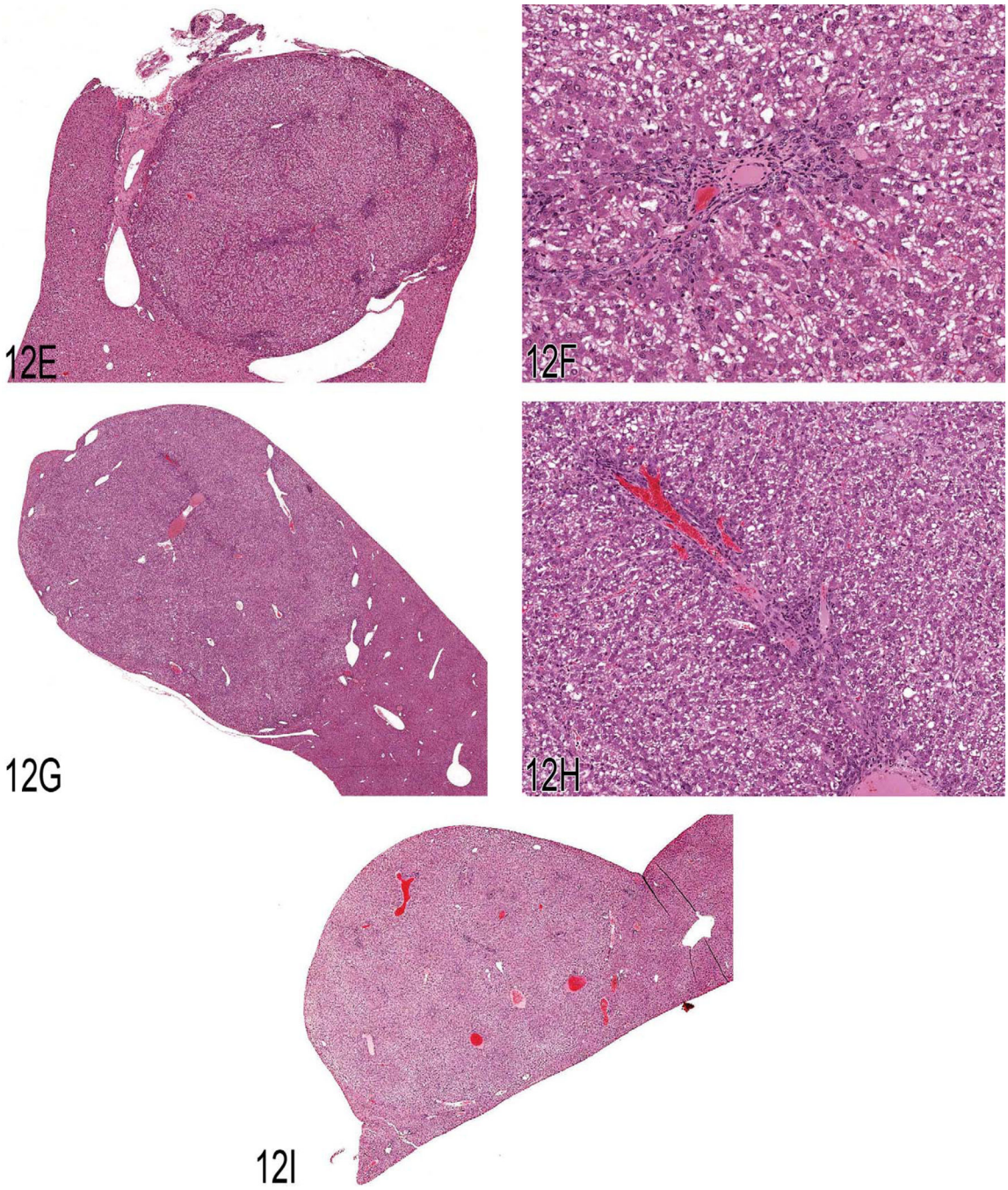

Figure 12.

(A) This image was projected at the 2008 NTP Satellite Symposium by Dr. Taki Harada and was presented as a representative example of a hyperplasia not associated with hepatotoxicity. The arrows show the edges of the hyperplastic lesion, which is tinctorially similar to the adjacent hepatic parenchyma. Multiple portal triads are present within this hyperplastic lesion. (B) An enlargement of the lower right quadrant of Figure 12A showing a portal triad just above the center of the image. Adjacent uninvolved hepatic parenchyma is present in the lower right corner of the photomicrograph. (C) This early example of focal

hyperplasia was provided by Dr. Harada. It is phenotypically similar to surrounding hepatic parenchyma and evident only because of its altered growth pattern and sinusoidal congestion. (D) Another example of a large area of hyperplasia similar to Figure 12A. Macrovesicular fat vacuoles are present within this lesion. (E) Case 1. A discrete nodular lesion from a treated male B6C3F1 mouse. The multiple areas of blue stippling within this nodule are portal triads. Because of the presence of the portal triads, the votes for diagnoses were split between focal hyperplasia and hepatocellular adenoma. (F) Case 1. A higher magnification of Figure 12A showing a portal triad within the nodular lesion. (G) Case 2. This nodular lesion from a treated male B6C3F1 mouse contained portal triads. Based on the voting, this lesion was considered a focus of cellular alteration. (H) Case 2. A higher magnification of Figure 12C showing a portal triad within the nodular lesion. (I) Case 3. This large, protruding mass was one of three seen grossly in the liver of the treated male B6C3F1 mouse. Portal triads were present within as well as at the periphery of this proliferative nodule. The voting clearly favored hepatocellular adenoma for this lesion.

Table 1

History of NTP satellite symposia.

Year	Location	Symposium theme
2009	Washington, DC	Tumor Pathology and INHAND Nomenclature
2008	San Francisco	Pathology Potpourri
2007	Puerto Rico	Pathology Potpourri
2006	Vancouver	Pathology of the Urinary System
2005	Washington, DC	Pathology of the Immune System
2004	Salt Lake City	Hepatic Pathology
2003	Savannah	An Exercise in Peer Review: The Pathology Working Group
2002	Denver	Techniques in Toxicologic Pathology
2001[a]		
2000	Phoenix	Establishing an NTP Database for Non-Neoplastic Lesions of Kidney and Urinary Bladder

[a] No symposium held in 2001.

Table 2

Incidence of spontaneous neoplasia in Tg.AC mice (*n* = 110 animals per sex per group).

	Control		TPA positive control	
	Male	**Female**	**Male**	**Female**
Skin				
Papilloma	1	1	92	96
Squamous cell carcinoma			7	2
Acanthosis/hyperplasia	14	20	55	43
Head				
Odontoma	5	4	5	7
Hematopoietic system				
Erythroleukemia		7	5	7

Abbreviation: TPA, 12-*O*-tetradecanoylphorbol-13-acetate.

Table 3

Selected criteria for myeloid hyperplasia versus granulocytic leukemia.

Myeloid hyperplasia	Granulocytic leukemia
All stages of granulocyte development	Immature cells predominate, various stages of granulocyte maturation absent
Erythropoietic activity present	Erythropoietic activity absent
Megakaryocytes numerous	Megakaryocytes few, present in organs where expected
Often associated with inflammation	Inflammation not usually present
Cells not invasive	Cells are invasive
Normal tissue of spleen relatively unaffected	Normal tissue of spleen is extensively replaced

Adapted from Long, Knutsen, and Robinson 1986.

Table 4

INHAND nomenclature criteria: Malignant oligodendroglioma.

Well-circumscribed lesion with a distinct border, extending over multiple areas of brain (spinal cord)
Characterized by focal or diffuse anaplasia, as evidenced by high cellularity, cellular atypia and pleomorphism, prominent proliferation of glomeruloid vessels at the tumor margins, nuclear polymorphism, increased mitotic index, necrosis, and/or meningeal infiltration
Atypical capillary endothelial hyperplasia (“garlands”), especially at the tumor periphery, is extensive and is a characteristic feature.
Necrosis with cystic changes and hemorrhages is frequent.

Table 5

INHAND nomenclature criteria: Special techniques for oligodenroglioma diagnostics.

Positive immunostaining for MBP has been reported in human and rat oligodendrogliomas and may be of use to confirm a diagnosis in the mouse.
Also, CNP may be a useful diagnostic aid in cases of less differentiated tumors.
Some human oligodendroglioma express S-100 and Leu-7 marker, but expression cannot be regarded as specific for oligodendrogliomas.
In ENU-induced gliomas in rats most of the oligodendrogliomas react with *Leu-7*, were negative for GFAP, usually S-100 negative; Vimentin was also generally negative but might be focally positive.
Neoplastic oligodendrocytes may stain positively for galactose cerebroside and carbonic anhydrase C.

Abbreviations: CNP, 2′, 3′-cyclic nucleotide 3′-phosphodiesterase; ENU, ethylnitrosourea; INHAND, International Harmonization of Nomenclature and Diagnostic Criteria for Lesions in Rats and Mice; MBP, myelin basic protein.

Table 6

INHAND nomenclature criteria: Benign oligodendroglioma.

Circumscribed lesion with a distinct border, confined to one major area of the central nervous system
Composed of sheets, rows, or nests of small uniform neoplastic cells with round, central, hyperchromatic nuclei and clear to lightly stained cytoplasm (perinuclear halo) with distinct cellular borders
Sheets of neoplastic cells are intersected by fibrovascular stroma.
Pronounced perinuclear halo is common with delayed fixation and results in the essentially artifactual but classically described “honeycomb” or “friedegg” cell pattern.
Prominent microvascular proliferation with atypical capillary endothelial hyperplasia can be extensive, especially at the periphery of the neoplasm.
Necrosis with cystic changes and hemorrhage with hemosiderosis may be present.
Other glial cells, such as astrocytes and transitional forms between oligodendrocytes and astrocytes, may be present in varying numbers.

Abbreviation: INHAND, International Harmonization of Nomenclature and Diagnostic Criteria for Lesions in Rats and Mice.

Table 7

INHAND nomenclature criteria: Malignant astrocytoma.

Indistinct border, diffusely infiltrating, sometimes multicentric, and extends over multiple brain (spinal cord) areas
Polymorphic appearance and high cellularity
Infiltrates along blood vessels (Virchow-Robin spaces)
Invasion into meninges, ependyma, and ventricles is common
Cells are generally round to fusiform, and have indistinct cell borders, cellular atypia, and pleomorphism. Cells may exhibit protoplasmic or fibrillary differentiation and prominent round or oval nuclei.
Neuronal cell bodies may persist within the neoplastic area.
Reactive astrocytes (gemistocytes) may be present.
Hemorrhage and necrosis may occur.
Necrosis with pseudopalisading is accompanied by marked cellular and nuclear pleomorphism of moderate to dense cellularity.

Abbreviation: INHAND, International Harmonization of Nomenclature and Diagnostic Criteria for Lesions in Rats and Mice.

Table 8

INHAND nomenclature criteria: Special techniques for astrocytoma diagnostics.

Neoplastic astrocytes of rodent brain do not react positively for GFAP, in contrast to astrocytomas from humans and domestic animals.
In most spontaneous gliomas of the rat, astrocytic cells reacting positively for GFAP may represent reactive rather than neoplastic astrocytes.
Chemically induced gliomas in rats contain GFAP-positive astrocytes that are neoplastic as well as reactive.
Multinucleated giant cells and vascular endothelial proliferation are not features of naturally occurring astrocytomas in the rat.

Abbreviations: GFAP, glial fibrillary acidic protein; INHAND, International Harmonization of Nomenclature and Diagnostic Criteria for Lesions in Rats and Mice.

Table 9

INHAND nomenclature criteria: Malignant glioma, mixed.

Indistinct border, mostly diffusely infiltrating, and present in multiple areas of the brain (spinal cord)
Polymorphic appearance, cellular atypia and pleomorphism is marked.
Multinucleated giant cells may be numerous.
Astrocytic or oligodendrocytic differentiation may not be obvious in some areas and some neoplasms.
Vascular proliferation is marked, and foci of necrosis and hemorrhage may be present.
Palisading of spindle-shaped cells around areas of necrosis may occur.
Bizarre mitotic figures may be present.

Abbreviation: INHAND, International Harmonization of Nomenclature and Diagnostic Criteria for Lesions in Rats and Mice.

Table 10

World Health Organization classification of meningiomas in domestic animals.

Meningotheliomatous
Fibrous (fibroblastic)
Transitional (mixed)
Psammomatous
Angiomatous (angioblastic)
Papillary
Granular cell
Myxoid
Anaplastic (malignant)

Source: Koestner et al. 1999.

Table 11

Proposed diagnostic criteria for myxoid meningiomas in mice.

Meningioma composed of spindle-to stellate-shaped cells with scant cytoplasm embedded in a predominantly myxomatous matrix. Alcian blue positive, Masson's trichrome negative
May be benign or malignant

Table 12

Proposed diagnostic criteria for psammomatous meningiomas in rats.

Meningioma composed of lobules and small whorls of neoplastic epithelioid cells intermixed with numerous small foci of hyalinized collagen and mineralization (“Psammoma bodies”)
“Psammoma bodies” often occur in the centers of the lobules.
Neoplastic cells have indistinct cell margins and variable amounts of amphophilic to pale eosinophilic cytoplasm.

Table 13

Diagnostic features of pulmonary mucous cell metaplasia.

Mucus-containing spaces lined predominantly by a single layer of mature mucous cells covering alveolar walls in the lung periphery
Very low mitotic activity
PAS/Alcian blue-staining enhances identification of mucous cells and mucus.
Usually accompanied by features of chronic inflammation and fibrosis
Proliferation of other epithelial elements as described for bronchiolo-alveolar hyperplasia can be present
Background of normal bronchiolo-alveolar architecture retained to various degrees, depending on amount of associated inflammation and fibrosis

Abbreviation: PAS, periodic acid–Schiff.